JCI insight

Integrin-Kindlin3 requirements for microglial motility in vivo are distinct from those for macrophages

Julia Meller, … , Bruce D. Trapp, Tatiana V. Byzova

JCI Insight. 2017;2(11):e93002. https://doi.org/10.1172/jci.insight.93002.

Research Article **Cell biology** **Neuroscience**

Microglia play a critical role in the development and homeostasis of the CNS. While mobilization of microglia is critical for a number of pathologies, understanding of the mechanisms of their migration in vivo is limited and often based on similarities to macrophages. Kindlin3 deficiency as well as Kindlin3 mutations of integrin-binding sites abolish both integrin inside-out and outside-in signaling in microglia, thereby resulting in severe deficiencies in cell adhesion, polarization, and migration in vitro, which are similar to the defects observed in macrophages. In contrast, while Kindlin3 mutations impaired macrophage mobilization in vivo, they had no effect either on the population of microglia in the CNS during development or on mobilization of microglia and subsequent microgliosis in a model of multiple sclerosis. At the same time, acute microglial response to laser-induced injury was impaired by the lack of Kindlin3-integrin interactions. Based on 2-photon imaging of microglia in the brain, Kindlin3 is required for elongation of microglial processes toward the injury site and formation of phagosomes in response to brain injury. Thus, while Kindlin3 deficiency in human subjects is not expected to diminish the presence of microglia within CNS, it might delay the recovery process after injury, thereby exacerbating its complications.

JCI insight

RESEARCH ARTICLE

Integrin-Kindlin3 requirements for microglial motility in vivo are distinct from those for macrophages

Julia Meller,[1] Zhihong Chen,[2] Tejasvi Dudiki,[1] Rebecca M. Cull,[1] Rakhilya Murtazina,[1] Saswat K. Bal,[1] Elzbieta Pluskota,[1] Samantha Stefl,[1] Edward F. Plow,[1] Bruce D. Trapp,[2] and Tatiana V. Byzova[1]

[1]Department of Molecular Cardiology and [2]Department of Neuroscience, Lerner Research Institute, Cleveland Clinic, Cleveland, Ohio, USA.

Microglia play a critical role in the development and homeostasis of the CNS. While mobilization of microglia is critical for a number of pathologies, understanding of the mechanisms of their migration in vivo is limited and often based on similarities to macrophages. Kindlin3 deficiency as well as Kindlin3 mutations of integrin-binding sites abolish both integrin inside-out and outside-in signaling in microglia, thereby resulting in severe deficiencies in cell adhesion, polarization, and migration in vitro, which are similar to the defects observed in macrophages. In contrast, while Kindlin3 mutations impaired macrophage mobilization in vivo, they had no effect either on the population of microglia in the CNS during development or on mobilization of microglia and subsequent microgliosis in a model of multiple sclerosis. At the same time, acute microglial response to laser-induced injury was impaired by the lack of Kindlin3-integrin interactions. Based on 2-photon imaging of microglia in the brain, Kindlin3 is required for elongation of microglial processes toward the injury site and formation of phagosomes in response to brain injury. Thus, while Kindlin3 deficiency in human subjects is not expected to diminish the presence of microglia within CNS, it might delay the recovery process after injury, thereby exacerbating its complications.

Introduction

Among numerous cells in the CNS, microglia represent the most malleable and mobile cell type. Known to function as a surveillant and a main guard, microglia serve as a key regulator of development, homeostasis, and, as found recently, a central player in pathogenesis of a number of CNS diseases (1). In contrast to tissue macrophages that are recruited from blood, microglia originate from the yolk sack, migrate to the brain during early embryonic development, and play a key role in modulating neuronal circuits by pruning neurons and synapses. In the adult CNS, surveying "resting" microglia are evenly distributed within the brain and spinal cord, constantly screening surrounding tissue (2, 3). Microglia motility increases significantly in response to any perturbation within the CNS, including injury, breakdown of the blood-brain barrier, infection, or accumulation of pathological products, such as amyloid in Alzheimer's disease or sites of demyelination in multiple sclerosis (MS) (4). This often results in activation of microglia and mobilization to the sites of injury, a process known as microgliosis (5). Accumulation of microglial cells and their transformation into an "activated phenotype" are known to be neurotoxic in some cases and protective in others (1). Therefore, it is not surprising that recent studies have identified microglial responses as key determining factors in the pathogenesis in the vast majority of CNS pathologies, ranging from MS, Parkinson's disease, and Alzheimer's disease, to depression and schizophrenia (4, 6).

Together, it appears that the ability of microglia to sense and respond to the changes in their environment often determines the outcome in a number of developmental and pathological scenarios. However, how the motility of microglia is regulated, and whether its mechanisms are similar to those of monocytes/macrophages remains poorly understood. The ability of cells to interact with the extracellular environment and respond to changes depends heavily on the integrin family of transmembrane receptors. Integrins recognize virtually all components of the extracellular matrix (ECM) and mediate cell adhesion and migration. The main integrin on microglia is $\alpha_m\beta_2$ (also known as CD11b/CD18 integrin); it often serves as a marker for this cell type in the brain (7). Microglia also express β1 integrins, mainly $\alpha_4\beta_1$ and

Authorship note: J. Meller, Z. Chen, and T. Dudiki contributed equally to this work.

Conflict of interest: The authors have declared that no conflict of interest exists.

Submitted: January 24, 2017
Accepted: April 25, 2017
Published: June 2, 2017

Reference information:
JCI Insight. 2017;2(11):e93002. https://doi.org/10.1172/jci.insight.93002.

$\alpha_5\beta_1$, and a few members of the α_v integrin family (8). In respect to integrin expression, microglia and macrophages are similar, and most integrin-dependent functions are attributed to the main integrin $\alpha_m\beta_2$, which has been implicated in synaptic pruning (9) and mobilization and activation of microglia in autoimmune encephalomyelitis model (10).

In order to recognize extracellular ligands, integrins undergo "activation," resulting in transformation of inactive integrin into an active conformer, which is able to bind ligands and mediate cell adhesion (11, 12). Several studies have shown that the process of integrin activation depends on the presence of intracellular protein Kindlin (13). Additionally, other groups have demonstrated that another integrin activator, talin, is fully sufficient to promote integrin activation, even in the absence of Kindlin (14). Moreover, a recent study has shown that Kindlin might be crucial for integrin "clustering," rather than for inside-out integrin activation (15). At the same time, while Kindlins1 and 2 were shown to promote activation of β3 integrins, their activating effect on β1 integrins remains debated (16, 17). While the requirement for Kindlin to activate integrins and to mediate adhesion of certain immune cells has been well documented in vitro, its role in cell diapedesis and trafficking in vivo is less clear. A study focused on leukocyte motility in vivo demonstrated that Kindlin3 is indeed required for firm adhesion but is dispensable for leukocyte transmigration into the vessel wall (18). Together, the role of Kindlins and Kindlin3, in particular, in regulating cell motility in tissues rather than in vitro remains unclear.

The mechanisms underlying Kindlin functions are also still obscure. Via its FERM and PH domains, Kindlin has a capability to interact with a wide range of proteins and lipids (13). Indeed, the role of Kindlins is not limited to integrin binding and activation, as recent studies establish several integrin-independent functions of Kindlin2 (19). Thus, despite the fact that the direct interaction between Kindlin and its specific site on the integrin cytoplasmic domain has been documented, the functional requirement for this particular binding in cellular functions remain poorly understood.

One of the most prominent and recently identified problems in mechanistic and structural studies on integrins and their binding partners is a reliance on a very specific set of in vitro techniques using isolated transmembrane proteins and their fragments in the absence of appropriate membrane environment. As a result, a number of mechanistic conclusions have been developed outside of the cellular context, and these findings generate controversy. Another experimental drawback is an insufficient degree of Kindlin deletion in various cells and compensation by other Kindlins. Based on a recent study, 5% of total Kindlin3 level might be sufficient for its functionality (20).

Deficiency of Kindlin3 affects functions of three families of integrins (β1, β2, and β3) on circulating blood cells, thereby causing a life-threatening bleeding and immune disorder in humans (21). Knockout of Kindlin3 in mice leads to early postnatal lethality and recapitulates many of the complications caused by Kindlin3 deficiency in humans (22). Remarkably, Kindlin3-deficient patients experienced brain hemorrhaging complications, which often occurred in the absence of obvious injury. Moreover, these complications were more severe than in Glanzmann thrombasthenia patients with a lack of platelet integrins or leukocyte adhesion deficiency (LAD) patients lacking integrins on leukocytes. This suggests that Kindlin3 deficiency might affect other cell types in the brain, most likely microglia, whose mobility plays a key role in injury responses.

Although many studies do not discriminate between microglia and monocyte-derived macrophages, evidence that microglia constitute a very different cell type is no longer based merely on distinctions in ontogenesis and the renewal mechanisms. The gene expression signature of microglia in vivo was shown to be unique and not present in either microglial or macrophage cell lines (23). Based on these studies, it is inappropriate to apply the conclusions derived from macrophages or cell lines to microglia.

A thorough in vivo–based study demonstrated that microglia are characterized by a different pattern of gene expression and differential responses to the same inflammatory environment of an MS model compared with monocyte-derived macrophages (24). It was shown that monocyte-derived macrophages are highly inflammatory and appear to initiate demyelination in MS, whereas resident microglia primarily clear debris (24). The study suggests that new therapeutic strategies should discriminately target infiltrating monocytes while preserving tissue-resident microglia.

The aim of the present study is to compare the migratory characteristics of macrophages to those of resident microglia and determine the requirements for integrin/Kindlin signaling for this process in vitro and in vivo. To directly assess whether Kindlin3 and its direct binding to the integrin cytoplasmic domain are required for integrin inside-out or outside-in signaling and, most importantly, for the motility of these immune cells in vitro and in vivo, we generated a microglia-specific Kindlin3-knockout

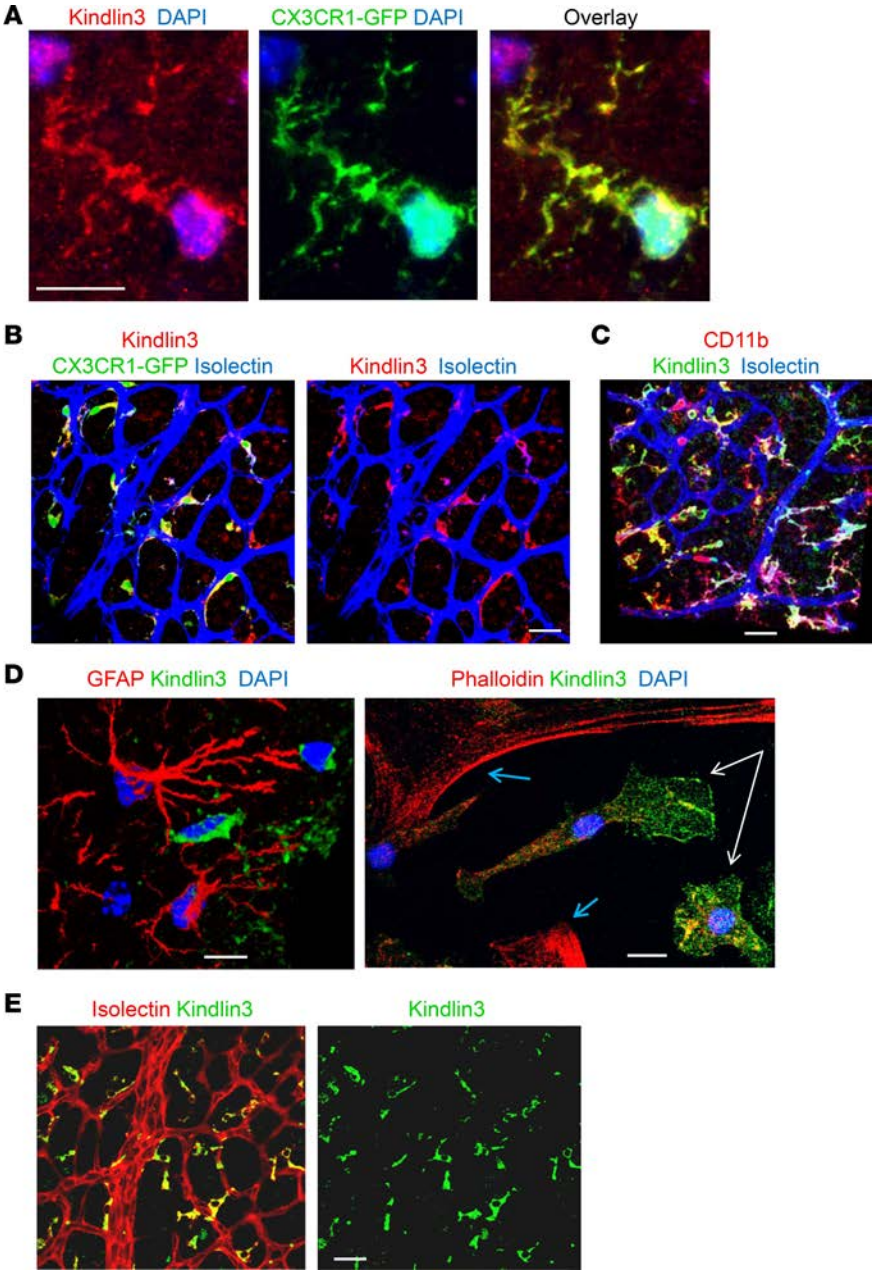

Figure 1. Kindlin3 is expressed in microglia in vitro and in vivo. (**A**) Brain tissue from P9 *Cx3cr1*$^{GFP/+}$ mice was stained for Kindlin3. Representative confocal image from the cortical region showing expression of Kindlin3 (red), GFP (green), and overlay (right), with nuclei shown in blue. Scale bar: 10 μm. (**B**) Projection of z-stack images showing Kindlin3 in whole-mount retinas from P9 Cx3cr1$^{GFP/+}$ mice (Kindlin3, red; GFP, green; isolectin, blue). Scale bar: 100 μm. (**C**) 3D reconstitution of an image stack from P7 whole-mount retinas showing coexpression of CD11b (red) and Kindlin3 (green) within the same cells. Blood vessels are in blue (isolectin). Scale bar: 100 μm. (**D**) 3D reconstitution of a brain slice from the cortical region (left)showing lack of Kindlin3 expression (green) in GFAP-positive cells (red). Staining of cultured astrocytes and microglial cells (right) showing lack of Kindlin3 expression (green) in astrocytes (actin-rich cells predominantly stained with phalloidin, red). Nuclei are shown in blue. Scale bar: 10 μm. (**E**) P7 whole-mount retinas stained for Kindlin3 (green) and blood vessels (isolectin, red). Scale bar: 100 μm.

(K3KO) and Kindlin3-knockin mice harboring QW→AA mutations in the F3 domain of *Kindlin* (K3KI), which disable direct Kindlin interaction with several integrins (25). We analyzed the consequences of Kindlin3 deficiency on microglia compared with monocyte-derived macrophages and demonstrate that, while in vitro migration defects of isolated microglia are comparable to those of macrophages, the effects of Kindlin3 loss on in vivo migration of these cell populations are strikingly different.

Results

Kindlin3 is exclusively expressed in microglia of the brain and retinal origin. To assess Kindlin3 expression in microglia and other cell types in the CNS, we took advantage of a mouse model, in which GFP expression is driven by the fractalkine receptor *Cx3cr1* promoter, which is expressed exclusively by microglia in the postnatal CNS (4). Analysis of cerebral cortical tissue sections at P9 revealed that CX3CR1-GFP–expressing cells were positive for Kindlin3 (Figure 1A). The cells had typical microglial morphology, with characteristic extensions or processes (Figure 1A). No detectable Kindlin3 expression was found in other cells in the brain. This was confirmed in retinas, in which all CX3CR1-GFP–expressing cells were Kindlin3 positive (Figure 1B). Moreover, all Kindlin3-positive cells also expressed CD11b, the α subunit of integrin $\alpha_m\beta_2$, which serves as a microglia marker (Figure 1C). Brain astrocytes identified by GFAP staining (26) did not express Kindlin3, as evidenced by costaining of brain tissue sections or mixed cultures of microglia and astrocytes (Figure 1D). Thus, Kindlin3 was almost exclusively expressed by microglia, both in retinas (Figure 1E) and the brain.

Based on literature, the predominant integrin expressed by microglia is $\alpha_m\beta_2$. Microglia also express β1 and a very low level of β3 integrins. Analysis of β1 and β2 integrin expression on WT and K3KI microglia revealed that QW→AA mutations within Kindlin3 did not reduce the expression of these integrins based on immunostaining and flow cytometry (Supplemental Figure 1, A and B; supplemental material available online with this article; https://doi.org/10.1172/jci.insight.93002DS1).

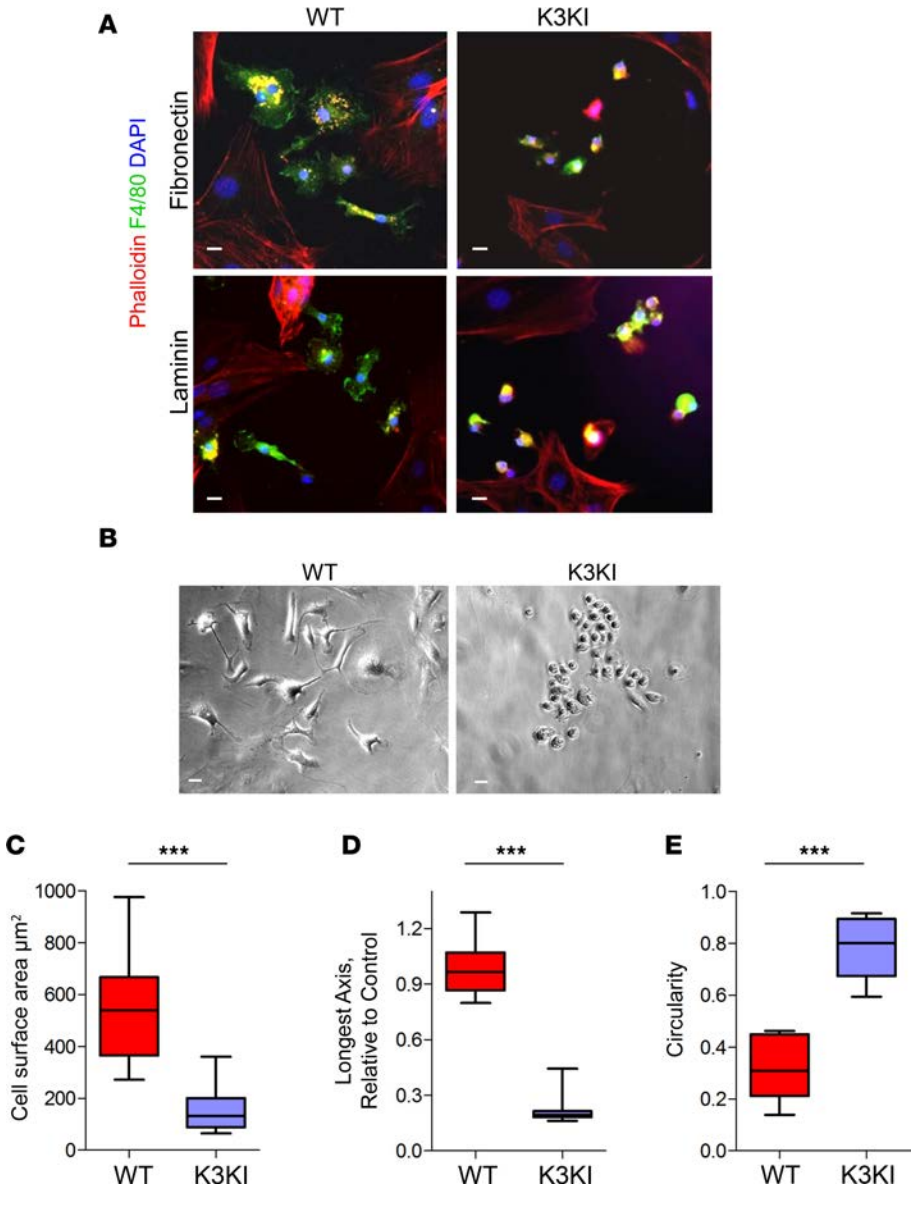

Figure 2. Impaired cell spreading and front-to-back cell polarity in Kindlin3 mutant microglia. (**A**) Mixed astrocytes and microglia from WT and Kindlin3 mutant knockin (K3KI) mice were plated on fibronectin or laminin for 24 hours and stained for F4/80 (green) and filamentous actin (phalloidin, red). Images show impaired cell spreading of microglia from K3KI mice. Note that spreading of astrocytes is not affected by Kindlin3 mutation. Scale bar: 10 µm. (**B**) Phase-contrast image showing brain microglia from WT and K3KI mice. Microglial cells were isolated from mixed brain culture by removal of astrocytes with trypsin, as described in Methods. Kindlin3-deficient microglia adherent to astrocyte-deposited ECM display lack of lamellipodia, reduced cell spreading, and loss of front-to-back cell polarity. Scale bar: 10 µm. (**C**–**E**) Quantification of cell-spreading area, circularity, and longest axis in purified microglial cells (n = 15 per group from 3 independent experiments). ***$P < 0.001$, 1-tailed Student's t test. Box-and-whisker plots show median (line within box), upper and lower quartiles (bounds of box), and minimum and maximum values (bars).

Kindlin3-integrin interaction is essential for microglia spreading and polarity. Next, microglia were isolated from brain tissue and identified by positive staining for F4/80, another myeloid cell marker, which stains microglia exclusively (as well as macrophages) but not astrocytes or other cells present in microglial culture from the brain (Figure 2A). As shown in Figure 2A, WT microglia displayed substantial adhesion and spreading when replated on ECM proteins, as exemplified by fibronectin and laminin, key representative ligands for β1 integrins. In contrast, K3KI microglia were not able to spread on either fibronectin or laminin. Notably, K3KI mutations did not affect adhesion or spreading of the astrocytes present in the microglial cultures, consistent with the lack of Kindlin3 expression by astrocytes. In mixed microglia-astrocyte cultures, K3KI microglia were not able to spread on astrocyte-produced ECM (Figure 2B). As a result, the K3KI cell area was several times smaller than that of WT cells spread on astrocyte matrix, for which fibronectin serves as a main ligand (Figure 2C). Likewise, change in cellular morphology upon spreading was substantially reduced in K3KI cells compared with WT microglia, as measured by cell length (Figure 2D) and circularity (Figure 2E).

Next, we assessed the consequences of the complete knockout of Kindlin3 in microglia. Microglial cells were isolated from mice expressing floxed *Kindlin3* ($K3^{lox/lox}$) and infected with adenovirus encoding Cre-recombinase to initiate Kindlin3 excision. As shown in Figure 3A, Cre-adenovirus infection (but not control adenovirus infection) induced the loss of cell adhesion and spreading, eventually leading to rounding and detachment of nearly 100% of cells plated on fibronectin. Image analysis revealed that the longest axis of individual cells treated with Cre-encoding adenovirus was decreased by 3-fold compared with untreated cells, whereas control GFP-encoding virus (also used as transfection efficiency control) had a negligible effect (Figure 3B). Likewise, GFP-encoding adenovirus treatment caused minimal cell rounding, as shown by measurements of cell circularity in Figure 3C. At the same time, cells treated with Cre-encoding adenovirus were almost round, with an average circularity index of 0.85, as compared with

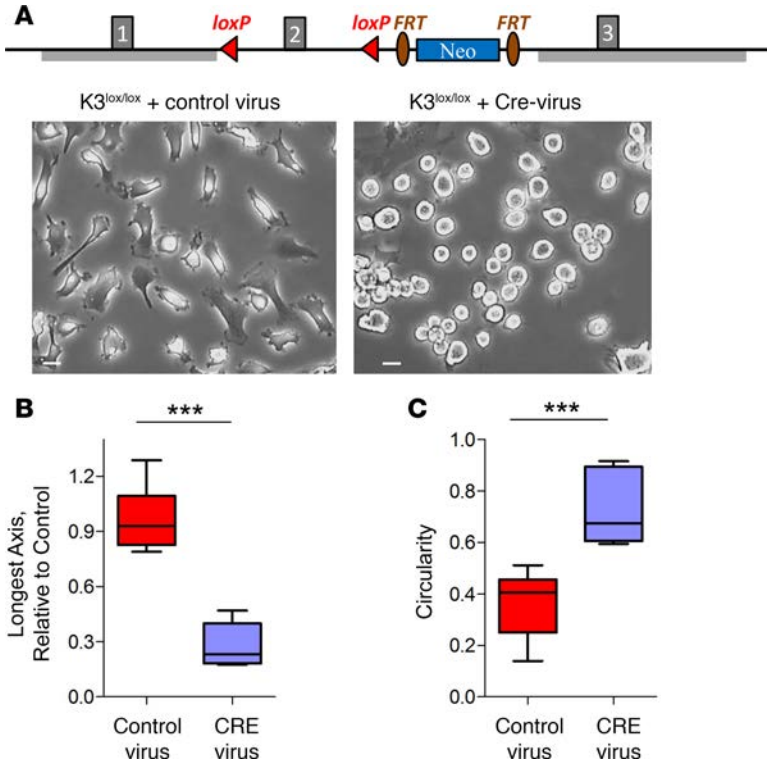

Figure 3. Kindlin3 excision in microglia leads to the loss of cell adhesion and spreading. (**A**) Scheme illustrating generation of *Kindlin3*$^{lox/lox}$ mice (top). Microglial cells isolated from *Kindlin3*$^{lox/lox}$ mice were infected with either control adenovirus (bottom left) or Cre-encoding adenovirus (bottom right) to delete Kindlin3. Images show cell-spreading impairment in Cre-expressing microglia. Scale bar: 10 μm. (**B** and **C**) Quantification of longest axis and circularity in virus-infected microglial cells (n = 10 per group from 2 independent experiments). ***$P < 0.001$, 1-tailed Student's t test. Box-and-whisker plots show median (line within box), upper and lower quartiles (bounds of box), and minimum and maximum values (bars).

untreated cells, with a circularity index of 0.35 Thus, Kindlin3 excision in microglia leads to the loss of cell adhesion and spreading on β1 integrin ligands. Together, these results indicate that knockout of Kindlin3 and QW→AA mutations within Kindlin3 resulted in a similar loss of cell adhesiveness and spreading.

Kindlin3-integrin interaction controls both inside-out and outside-in integrin signaling in microglia. Next, we assessed whether treatment with Mn^{2+}, which is known to bypass the requirement for inside-out integrin activation, is able to induce binding of fibrinogen, a ligand for three different subfamilies of integrins (β1, β2, and β3). As shown in Figure 4A, treatment with Mn^{2+} promoted fibrinogen binding to both WT and K3KI microglia. Thus, Mn^{2+} is able to activate integrins on K3KI microglia, even in the absence of a direct Kindlin3-integrin interaction. Next, we stained WT and K3KI microglia with 9EG7 antibody, which recognizes the activated (and occupied) conformer of β1 integrin. Mn^{2+} increased 9EG7 staining of both WT and K3KI cells (Figure 4B), thereby demonstrating that β1 integrin can be exogenously activated on K3KI cells.

During development and in numerous CNS pathologies, microglia are activated by a complement system and by neuron-derived fractalkine acting through its receptor, CX3CR1, which is exclusively expressed by microglia in CNS. Therefore, we used these key physiological microglia agonists to stimulate microglia adhesion and spreading (Figure 4C). Activation with complement components C5a and fractalkine induced cell spreading of WT microglia, and the area of adherent cells increased by more than 2-fold (Figure 4C). In contrast, neither C5a nor fractalkine were able to induce spreading of K3KI microglia (Figure 4C), indicating that Kindlin3-integrin binding is required for microglia activation by physiological agonists. Likewise, treatment with Mn^{2+} to bypass inside-out integrin activation induced spreading of WT cells but failed to promote spreading of K3KI microglia. Thus, despite promoting β1 integrin activation, Mn^{2+} treatment failed to induce the spreading of K3KI microglia on fibronectin as compared with WT cells (Figure 4C). This indicates that a QW→AA mutation within Kindlin3 affects microglia spreading, even when integrins are forced to assume "unbent" or active conformation by Mn^{2+} stimulation, demonstrating a role of Kindlin3-integrin interactions in outside-in integrin signaling.

Kindlin3-integrin interaction coordinates front-to-back cell polarity in migrating microglia. Integrin activation followed by ligation triggers a series of post-ligand-binding events, resulting in formation of adhesion complexes bridging the cytoskeleton with ECM at the leading edge of migrating cells (27). One of the first signaling events is recruitment of focal adhesion kinase (FAK) to sites of new integrin adhesions and subsequent phosphorylation of FAK. Treatment of WT microglia with Mn^{2+} induced activation of β1 integrin, as evidenced by 9EG7 staining (Figure 4, B and D), followed by at least a 2-fold increase in phosphorylation of FAK at Y397 (Figure 5B). In contrast, in K3KI microglia, Mn^{2+} promoted β1 integrin activation, but not FAK phosphorylation (Figure 4B and Figure 5B), indicating that the interaction between Kindlin3 and integrin is essential for initiation of adhesion assembly mechanism. In freshly adherent cells, most of the FAK in WT, but not in K3KI, microglia was phosphorylated and localized in adhesion complexes (Figure 5).

Microglial cells are highly polarized cells with a distinctive pattern of FAK recruitment and phosphorylation profile: while phosphorylated FAK was present at the leading edge and front ruffles of the cell, nonphos-

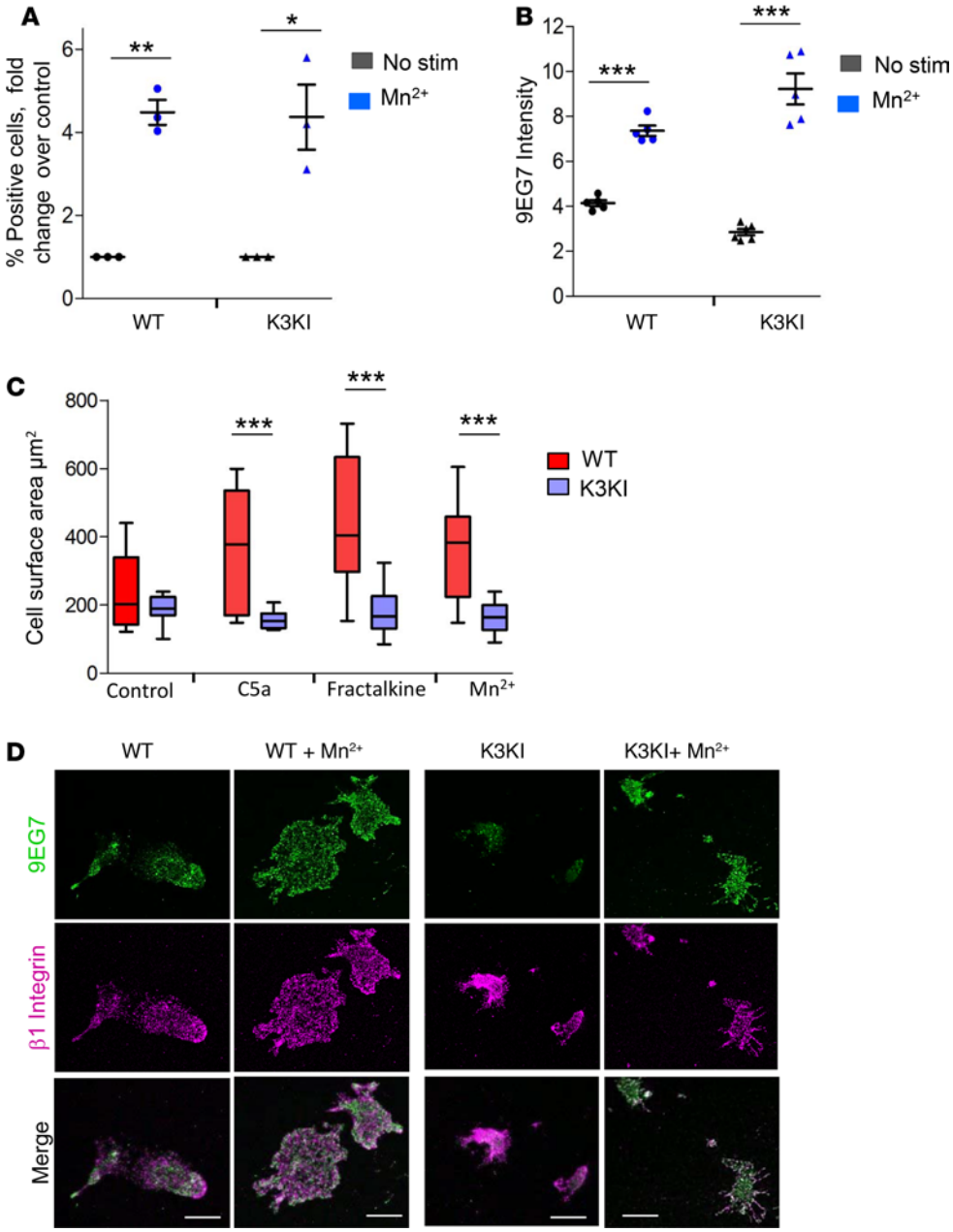

Figure 4. Mn^{2+} activates integrins in Kindlin3-knockin microglia but fails to induce outside-in signaling. (**A**) Microglial cells from WT and Kindlin3 mutant knockin (K3KI) mice were tested for ability to bind soluble fibrinogen (FG) with or without $MnCl_2$ (1 mM) as described in Methods. Flow cytometry analysis of FITC-conjugated FG binding shows a 4-fold increase in the percentage of cells positive for FG binding in both WT and K3KI mice after stimulation with Mn^{2+} (mean ± SEM from $n = 3$ independent experiments using a total of 8 mice per group). (**B**) Representative quantification of 9EG7 binding with and without 5-minute $MnCl_2$ stimulation (mean ± SEM from $n = 5$ cells per group of 4 independent experiments). (**C**) Analysis of cell-spreading area. Microglia from WT and K3KI mice were plated on fibronectin and incubated with C5a (10 ng/ml), fractalkine (200 ng/ml), or $MnCl_2$ (1 mM) for 50 minutes. Both chemokines and Mn^{2+} enhanced cell spreading in WT microglia but not in K3KI microglia ($n = 10$ cells per group from 3 independent experiments). (**D**) Microglial cells from WT and K3KI mice were plated on fibronectin for 2 hours and stained for active β1 integrin (clone 9EG7, green) and total β1 integrin (magenta). Scale bar: 5 µm. Box-and-whisker plots show median (line within box), upper and lower quartiles (bounds of box), and minimum and maximum values (bars). $^*P < 0.05$, $^{**}P < 0.01$, $^{***}P < 0.001$, 1-tailed Student's t test.

phorylated FAK was present throughout the cell body and its trailing edge (Figure 6, A and B). Quantification of phospho-Y397FAK distribution revealed that in WT microglia the level of phospho-Y397FAK at the leading edge of the cell was at least 10 times higher compared with its trailing end, whereas total FAK was equally distributed (Figure 6C). In contrast, in K3KI microglia phospho-Y397FAK was enriched at the cell edges but the front-to-back polarization was absent, indicating the failure of molecular clutch initiation. Moreover, even at the edges of K3KI cells, the levels of phospho-Y397FAK were several times lower compared with WT cells (Figure 6A). The lack of cell polarity in K3KI cells was confirmed by staining for Ser19-phosphorylated myosin light chain (pMLC), which normally highlights contractile areas (28). As anticipated, pMLC was predominantly localized at the trailing edge of WT cells (Figure 7, A and B). In contrast, in K3KI cells pMLC was evenly distributed within the cytoplasm, without any hints of polarization. This indicates that Kindlin3's interaction with the integrin cytoplasmic domain is required for integrin outside-in signaling and cell polarization.

A characteristic feature of microglia is the formation of circular structures, i.e., podosomes, which are crucial for ECM degradation during microglial migration (29). Podosomes can be visualized in vivo and in vitro by staining for ionized calcium–binding adaptor molecule 1 (Iba1), a microglia-specific calcium-bind-

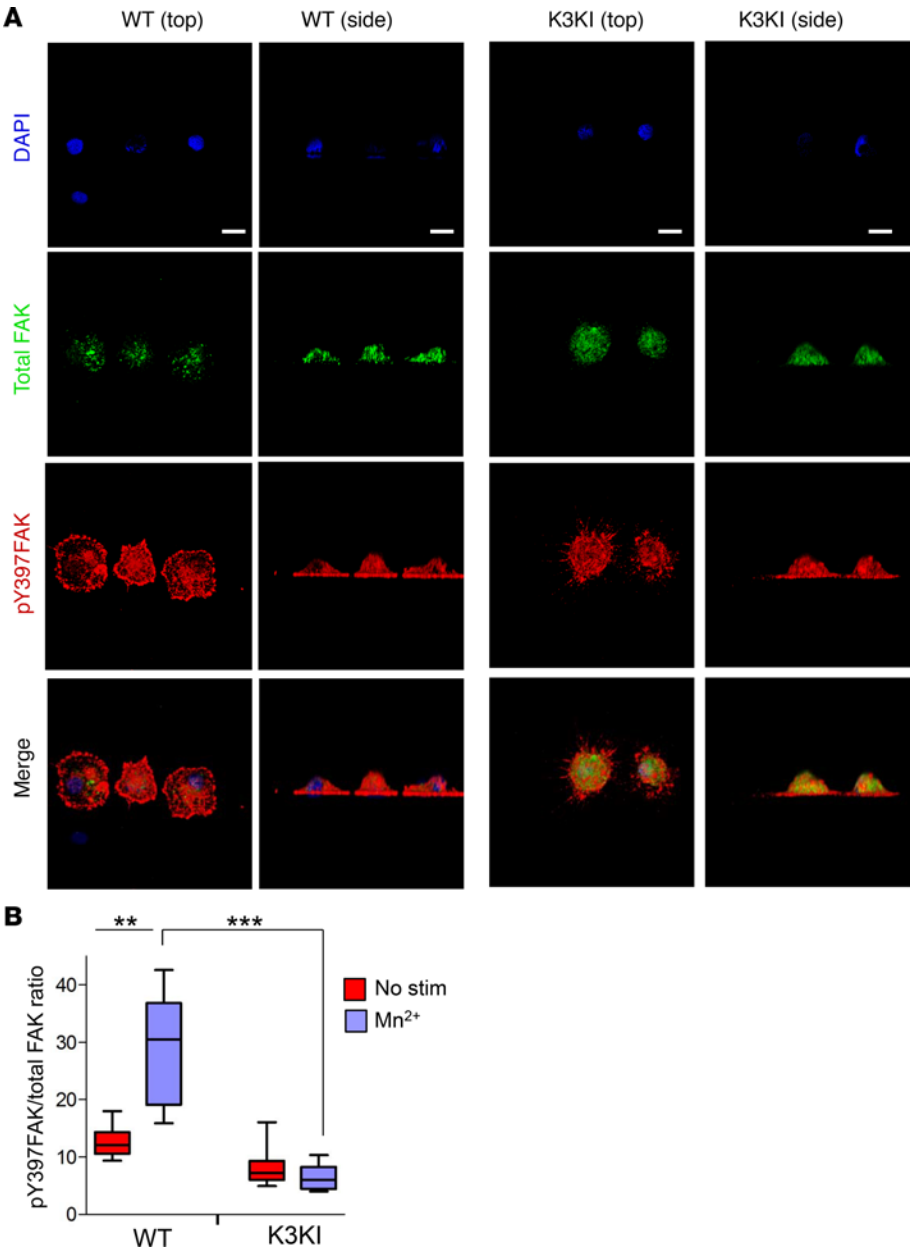

Figure 5. Integrin activation fails to induce focal adhesion kinase phosphorylation in K3KI microglia. (**A**) Staining for phospho-Y397 focal adhesion kinase (pY397FAK) and total FAK of microglia plated on fibronectin (FN) for 1 hour. Scale bar: 10 μm. (**B**) Quantification of pY397 FAK to total FAK ratio in microglia plated on FN that were either stimulated with Mn^{2+} or left untreated (No stim) (n = 30 from 2 experiments). Box-and-whisker plots show median (line within box), upper and lower quartiles (bounds of box), and minimum and maximum values (bars). $^{**}P < 0.01$, $^{***}P < 0.001$, 1-tailed Student's t test.

ing protein involved in actin bundling (30). Indeed, staining of isolated microglia for Iba1 revealed that more than 50% of WT cells have recognizable round podosomes (Figure 7C). These structures were completely absent in K3KI microglia. Together, these findings establish that direct binding of Kindlin3 to integrins is critical for signaling events resulting in podosomes formation, which is anticipated to halter critical functions for these cells.

Lack of Kindlin3-integrin interaction completely abolishes the ability of microglia to migrate in vitro. Activated microglia are characterized by high motility and an easily identifiable leading edge with ruffling membranes and trailing ends (front-to-back polarity) (Supplemental Videos 1 and 2 and Figure 8A). WT microglia cultured on astrocyte-deposited ECM moved at an average velocity of approximately 12 μm per minute (Supplemental Video 1 and Figure 8B). In contrast, K3KI microglial cells remained round and unpolarized, i.e., lacking identifiable front or back, and immobile under the same conditions (Supplemental Video 2 and Figure 8, A and B). While certain feeble movement of membrane ruffles was observed at the edges of the cells, no visible protrusions were apparent. K3KI cells were failing to engage their integrins. This is a likely consequence of abnormalities in "molecular clutch" initiation. Thus, our results showed that K3KI cells were immobile on astrocyte-deposited ECM (Supplemental Videos 1 and 2 and Figure 8, A and B). Assessment of chemotactic migration toward complement derived chemoattractant C5a also showed a dramatic reduction in K3KI microglia motility compared to WT cells. Thus K3KI cells are incapable of random or integrin mediated directed migration (Figure 8C).

In vitro consequences of Kindlin3 deficiency are comparable between microglia and monocyte-derived macrophages. Since macrophages express similar integrin repertoires and are considered to be similar to microglia, we performed ex vivo analysis of cell migration using freshly isolated peritoneal macrophages from WT and K3KI mice. As shown in Figure 9, A and B, more than 65% of WT macrophages were adherent and spread on fibronectin. At the same time, 95% of the K3KI macrophages did not spread. Further, WT macrophages showed a clear polarization (measured as the ratio of the longest axis of the cell to its shortest axis), while K3KI cells did not polarize (Figure 9C). Cell spreading and adhesion were rescued in Kindlin3-deficient macrophages transfected with EGFP-*Kindlin3* (Figure 9,

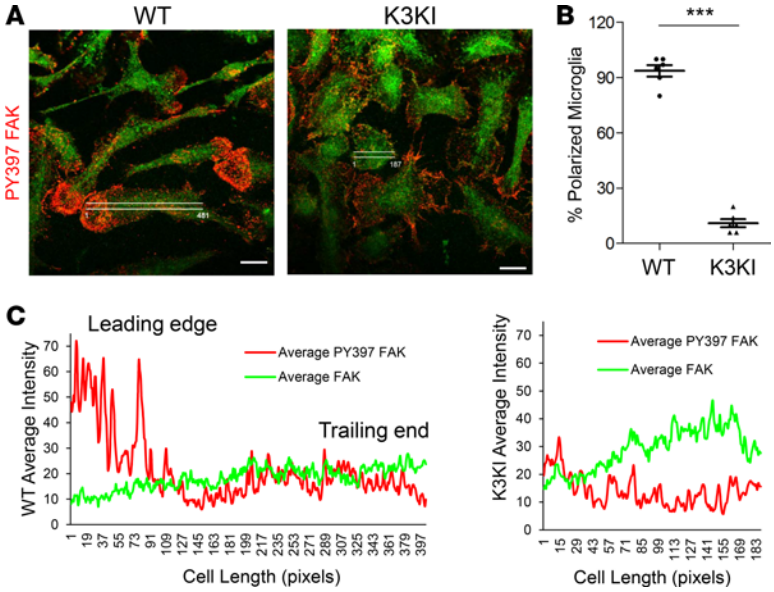

Figure 6. Kindlin3 is required for focal adhesion kinase recruitment and phosphorylation. (**A**) Microglial cells stably adherent to fibronectin (FN) from WT and Kindlin3 mutant knockin (K3KI) mice stained for phospho-Y397 focal adhesion kinase (pY397FAK) (red) and total FAK (green). Scale bar: 10 μm. (**B**) Over 95% of the WT microglia are polarized (measured as the ratio of the longest axis of the cell to its shortest axis) in comparison to 10% of K3KI microglia (mean ± SEM from n = 6 independent experiments with 30 cells counted/group/experiment). ***$P < 0.001$, 1-tailed Student's t test. (**C**) Average fluorescent intensities for WT and K3KI mice measured over a line profile for each antigen (as described in Methods), starting from the leading edge (pixel 1) (n = 3). In WT cells, FAK is predominantly phosphorylated on Y397 at the leading edge, but K3KI cells show diffused Y397 FAK phosphorylation.

D and E). Then, macrophage motility on fibronectin was measured using the Oris migration device. WT macrophages almost completely populated the detection zone, while the K3KI macrophages showed over a 3-fold decrease in the area of migration (Figure 9F). These results are consistent with the findings of Klapproth et al. (20) for neutrophils and leukocytes.

Kindlin3 deficiency diminishes in vivo macrophage migration. Next, we assessed how Kindlin3 mutation affected migration and recruitment of macrophages into inflammatory sites in vivo using a thioglycolate-induced peritonitis model. Peritoneal macrophages were collected 48 hours after thioglycolate injection and quantified. As shown in Figure 9G, macrophage transmigration into the peritoneal cavity was reduced by 50% in K3KI mice as compared with WT mice, thereby demonstrating that Kindlin3 is required for in vivo macrophage migration and recruitment. This is similar to the defects observed in Kindlin3-deficient neutrophils and leukocytes (20).

Microglial migration and population of CNS during development is not affected by Kindlin3 mutations. Unlike macrophages, resident microglia originated from the yolk sac during early embryogenesis; they then migrate and complete the population of CNS in midgestation. Microglia self-renew without contribution from infiltrating monocytes, thereby demonstrating their unique nature (31). Since the severe deficiency in cell migration might preclude the successful population of CNS by microglia, we compared the microglia distribution in WT and K3KI mice. As shown in Figure 10A, microglia visualized by Iba1 staining were present in brain and eye compartments of WT and K3KI mice at E13.5 at the similar density. To confirm this finding, K3KI and WT mice were crossed with the *Cx3cr1*$^{GFP/+}$ line, which allow specific microglia visualization (24) and imaging in live brain (2). As shown in Figure 10B, despite severe migration defects in vitro, K3KI microglia successfully populated brain tissue and appeared to be present in the adult brain at the levels similar to that of WT microglia.

The developing retina serves as another example of microglial migration in vivo. In mice, microglia inhabit the retina during the early postnatal period prior to the vasculature development (32). As shown in Figure 11A, no statistically significant difference was observed between numbers of CX3CR1-positive cells cross sections of WT embryo retinas compared with K3KI embryo retinas. Likewise, imaging and quantification of CX3CR1-positive cells in whole-mount retinas revealed no differences in microglia density between WT and K3KI mice either at P12 or in adulthood (P60) (Figure 11B). Therefore, using two distinct microglia-specific markers, Iba1 and CX3CR1, we show that, unlike macrophages, Kindlin deficiency and impaired integrin activation do not diminish microglial migration in vivo and population of CNS during development and early postnatal period.

Microglial mobilization and microgliosis in a MS model does not depend on Kindlin3-integrin axis. In adults, resident microglia are equally distributed in CNS tissues; they constantly probe and survey their environment by extending and retracting protrusions called processes (4). In healthy tissues, each microglial cell controls its own niche and rarely relocates its entire body. However, in inflammatory pathologies of CNS, exemplified by MS, microglia become activated and migratory, thereby leading to the redistribution of microglia

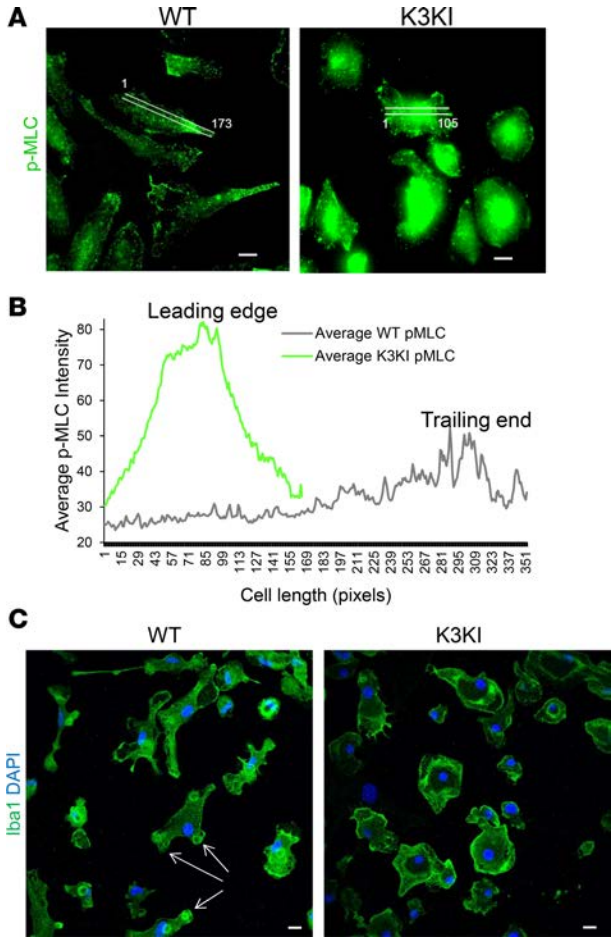

Figure 7. Absence of phospho–myosin light chain polarization and Iba1-positive podosome formation in Kindlin3 mutant microglia. (**A**) Phospho–myosin light chain (p-MLC) staining of stably adherent microglia. Representative line profiles (white lines labelled with their length in pixels) were used to measure fluorescent intensity from leading edge to trailing edge of cells. Scale bar: 10 μm. (**B**) Average fluorescent intensity for p-MLC staining from representative cells measured (n = 3) over a line profile for WT and K3KI mice from the leading edge (pixel 1) (as described in Methods). (**C**) Stably adherent microglial cells from WT and K3KI mice were stained for Iba1 6 hours after plating on fibronectin. Confocal images from the bottom cell surfaces show Iba1 localization to podosomal rings in WT cells but not in K3KI cells. Scale bar: 10 μm.

and their excessive accumulation in areas associated with demyelination (33). One of the models of MS is based on administration of the copper-chelator cuprizone, which causes consistent oligodendrocyte apoptosis and demyelination of white matter areas, notably the corpus callosum, which is followed by microglial migration and excessive accumulation, known as microgliosis (33, 34). In order to assess whether adult microglial migration in adult pathologies such as MS is affected by Kindlin deficiency, K3KI/*Cx3cr1*$^{GFP/+}$ and WT/*Cx3cr1*$^{GFP/+}$ mice were fed cuprizone-supplemented chow for 6 weeks, followed by staining and analysis of collected brain sections, with a focus on the corpus callosum, using CX3CR1-GFP and Iba1 for microglia visualization. As shown in Figure 12A, while microglia are evenly distributed within the healthy brain in both K3KI/*Cx3cr1*$^{GFP/+}$ and WT/*Cx3cr1*$^{GFP/+}$ mice, treatment with cuprizone caused uneven accumulation of microglia in select areas of corpus callosum. Surprisingly, no reduction in microgliosis was observed in cuprizone-treated K3KI/*Cx3cr1*$^{GFP/+}$ mice compared with WT/*Cx3cr1*$^{GFP/+}$ mice. The changes in microglia distribution pattern were assessed based on the numbers of microglial cells within a certain area (500 μM^2). In healthy brains, there were typically 1 to 2 cells present within this area, with a peak corresponding to 1 cell/field (Figure 12B). Cuprizone-induced microgliosis led to the drastic changes in this distribution pattern, which is characterized by two distinct peaks: one representing the areas devoid of microglia and a second peak identifying microglia clusters of more than 3 cells per field (Figure 12C). Although CX3CR1 was conclusively shown to be a selective marker of microglia but not infiltrated monocytes in CNS in general and during MS progression in particular (24), we further validated this finding using an alternative microglia marker, Iba1. As shown in Figure 13, there was no defect in migration and accumulation of Iba1-positive cells in K3KI mice as compared with WT mice.

Thus, Kindlin3 mutations, which cause a complete loss of integrin functions, microglia adhesion, and motility in vitro, do not diminish microglial mobilization and microgliosis in chronic inflammatory diseases of the CNS in adulthood, as exemplified by MS. This demonstrates that the mechanisms and requirement for in vivo migration of resident microglia are distinct from those of infiltrating macrophages, thereby emphasizing the unique nature of these resident immune cells.

Kindlin3 is required for an acute microglia response triggered by brain injury — implications for Kindlin3-deficient patients. While in the healthy brain microglial motility is restricted to random dynamic extensions and retractions of processes, microglia respond promptly to brain injury by rapid extension of microglial processes toward the injury site in order to prevent the diffusion of damaging degradation products released by injured neurons (35). In contrast to microglia movement in MS model, this is a rapid process, which is typically completed within an hour and does not involve the substantial repositioning of microglial cell. While several stimulators of this process, including ATP, have been identified, the intracellular regulators controlling this rapid response remain obscure. To determine the consequences of Kindlin3 deficiency on microglia response to acute injury, laser-induced focal brain injury was induced on both K3KI/*Cx3cr1*$^{GFP/+}$ and WT/*Cx3cr1*$^{GFP/+}$ mice and the movements of microglial processes toward the injury site were monitored using time-lapse multiphoton microscopy, a contemporary model for live analysis of microglia in the CNS (2, 36). In WT mice, the injury caused rapid redirection of protrusions

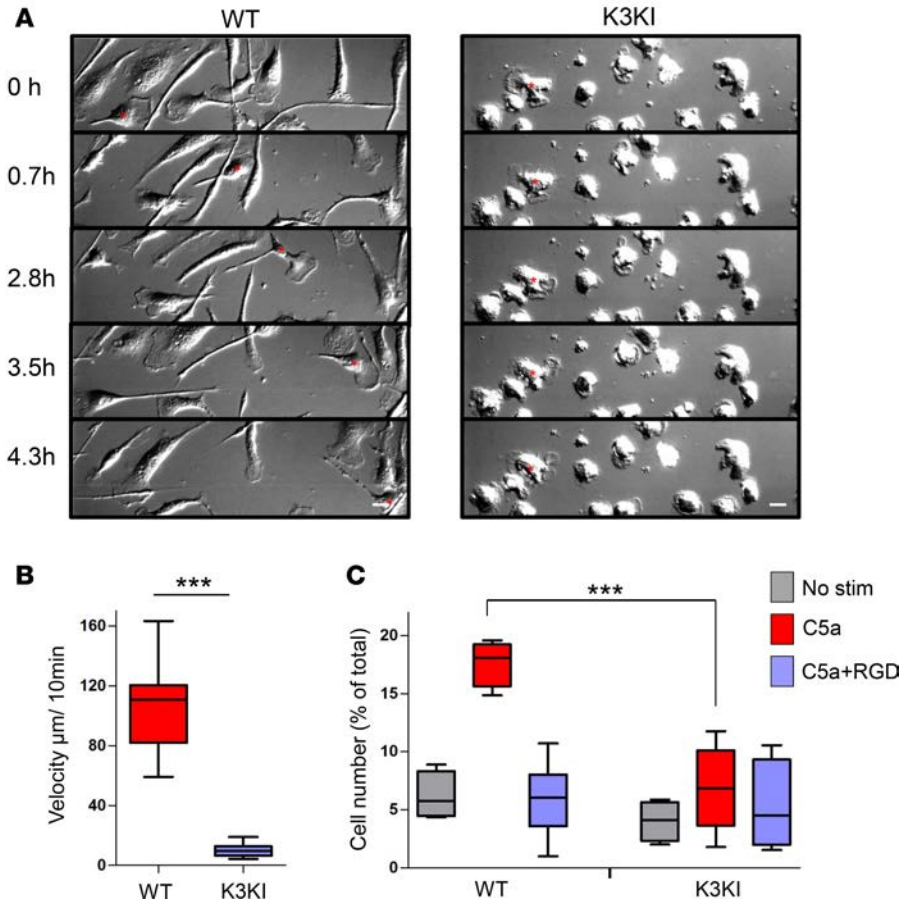

Figure 8. Kindlin3 is required for migration of microglial cells in vitro. (**A**) Random migration of microglia isolated from WT and Kindlin3 mutant knockin (K3KI) mice observed using differential interference microscopy. Time-lapse image sequence showing actively migrating WT microglia but not K3KI microglia (for the whole video, see Supplemental Videos 1 and 2). Scale bar: 10 μm. (**B**) Velocity of randomly migrating microglia was quantified with ImageJ software (n = 10 cells per group from 2 experiments). (**C**) C5a-induced chemotaxis of microglia was analyzed in a Transwell assay, as described in Methods (n = 4–9 fields per group from 3 experiments). Box-and-whisker plots show median (line within box), upper and lower quartiles (bounds of box), and minimum and maximum values (bars). ***$P < 0.001$, 1-tailed Student's t test.

from surrounding microglia toward the injury site. Growing protrusions then coalesced into a ring surrounding and rapidly isolating the scar (Figure 14A). While the initial response in redirecting the processes toward the injury was similar between WT/*Cx3cr1*$^{GFP/+}$ and K3KI/*Cx3cr1*$^{GFP/+}$ microglia, at later time points the movement velocity of K3KI/*Cx3cr1*$^{GFP/+}$ processes toward injury was substantially lower compared with WT/*Cx3cr1*$^{GFP/+}$ microglia (Figure 14A and Supplemental Videos 3 and 4).

Kymograph analysis of elongation of microglial processes in WT mice revealed a linear rate of approximately 1.1 μm per minute. In contrast, in K3KI mice the rate of extension of processes had two distinct phases: a first phase in which K3KI microglia had a comparable speed to that of WT microglia, and a second phase characterized by much slower rate of approximately 0.4 μm per minute (Figure 14, B and C). As a result, while WT microglia almost completely enclosed the injury site within the first 30 minutes, K3KI microglial processes extended at least 2 times slower, reaching a similar stage approximately 60 minutes after injury initiation. Thus, this analysis revealed that the Kindlin3-integrin interaction controls the extension velocity of microglial processes toward the injury site, which, in turn, might affect extent of tissue damage as well as and the timely recovery.

Two hours after the injury, microglia formed microglial phagosomes, which are known to be involved in engulfment and removal of damaged or dying neurons (35, 37). Defects and/or delays in phagosome formation are known to lead to defective engulfment and processing of damaged tissue, which, in turn, feeds back to neurological complications. Formation of these phagosomes continued for at least 9 hours after the injury (Figure 15A). These phagosomes were moving along extended microglial protrusions from the tips toward cell body transporting ingested material (Figure 15B), which is similar to previous reports (35). Compared with WT mice, the amount of phagosomes in K3KI mice was significantly reduced (Figure 15). Quantification of phagosomal structures 6 hours after the injury showed an at least 4-fold decrease in phagosome formation in K3KI mice as compared with WT controls (Figure 15C). Thus, Kindlin3-mediated signaling is critical for the mobilization of microglial processes, timely isolation of the injury site, and microglial phagosome formation. Thus, while Kindlin3 is dispensable for microglial cell migration in development and in an MS model, it is required for rapid responses of microglial protrusions during injury.

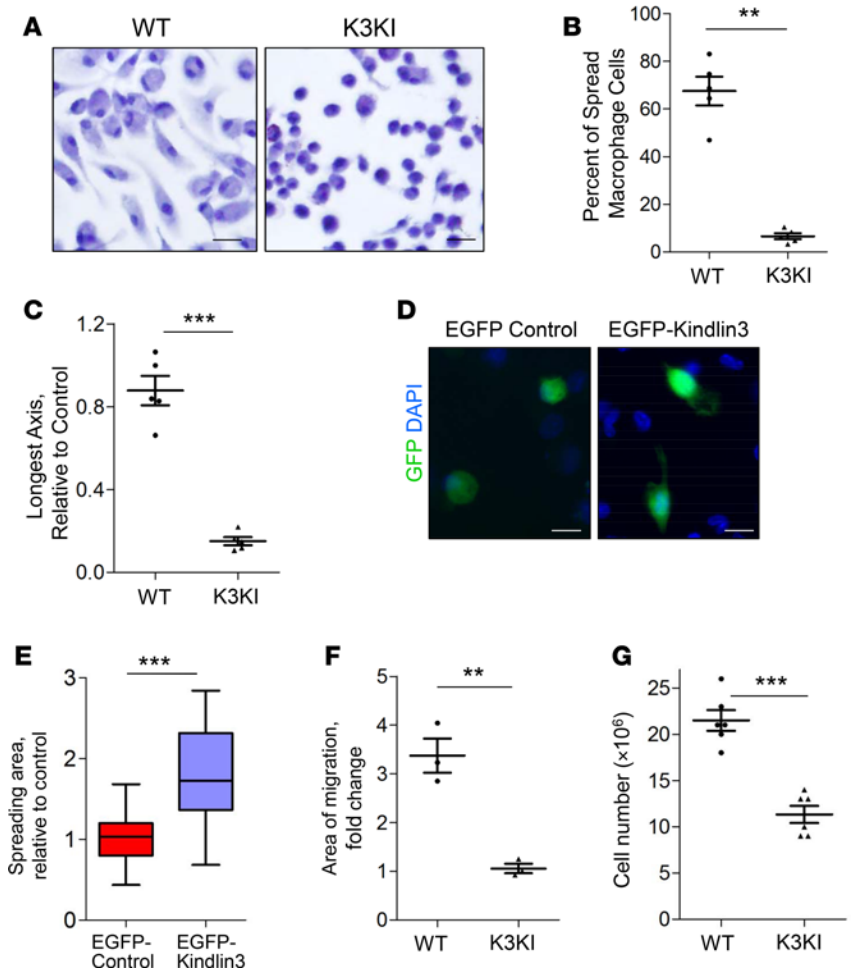

Figure 9. Kindlin3 mutant knockin macrophages exhibit defective spreading and migration in vitro as well as impaired recruitment to inflammatory sites in vivo. (**A**) 5×10^4 peritoneal macrophages were seeded per well, precoated with 10 μg/ml fibronectin for 24 hours, and stained with hematoxylin. The images show impaired spreading and lack of polarity in the Kindlin3 mutant knockin (K3KI) macrophages. Scale bar: 10 μm. (**B**) The number of polarized cells (cells with a ratio of the longest axis to shortest axis of 2:1 or greater) in both WT and K3KI mice was counted and is represented as the percentage of spread cells from $n = 5$ independent experiments, with 100 cells counted/group/experiment. (**C**) The average polarity of the K3KI cells shown as a measurement of their longest axis relative to WT cells ($n = 5$; mean ± SEM). (**D**) Spreading of Kindlin3-deficient macrophages was rescued by transfection with GFP-*Kindlin3* vector but not with the GFP vector alone. Scale bar: 10 μm. (**E**) Quantification showing a significant increase in the area of spreading by Kindlin3-deficient macrophages transfected with GFP-*Kindlin3* vector ($n = 22$ cells per group from 3 experiments). (**F**) In vitro cell migration assessed by the Oris cell migration assay. The quantification of cell migration represented as fold change in migration area, showing a significant reduction in migration by K3KI macrophages in comparison to WT macrophages (mean ± SEM, $n = 3$ independent experiments). (**G**) Peritoneal macrophages from WT and K3KI mice were collected after 72 hours of thioglycollate injection and counted with a hematocytometer. The graph shows a significant reduction in the number of cells accumulated in peritoneum of K3KI mice compared with WT mice (mean ± SEM, $n = 6$ per group). Box-and-whisker plots show median (line within box), upper and lower quartiles (bounds of box), and minimum and maximum values (bars). $^{**}P < 0.01$, $^{***}P < 0.001$, 1-tailed Student's *t* test.

Discussion

Using knockout and knockin models, this study establishes the role of the Kindlin-integrin interface in key microglia functions, including microglial migration and population of the CNS in development, microglial mobilization and microgliosis in chronic inflammatory disorders of CNS, i.e., MS, and timely response to acute injury. The lack of interaction between Kindlin3 and integrins in K3KI microglia resulted in defective integrin activation by key agonists, such as fractalkine and C5a, and led to severe abnormalities in adhesion, spreading, and migration of isolated brain microglia. The Kindlin3-integrin interaction was required for both inside-out integrin activation during adhesion and migration and integrin outside-in signaling in microglia, including FAK phosphorylation at the leading edge and actin rearrangement. Importantly, an exogenous integrin activator, $Mn2^+$, which bypassed the requirement for Kindlin3, restored integrin ligand binding but failed to rescue outside-in defects in K3KI microglia. Previous studies demonstrated that Kindlin3 is required for integrin function on platelets and leukocytes (21, 22, 38), while other studies show its role in integrin clustering but not initial ligand binding (39). This study is the first to our knowledge to demonstrate the requirement for Kindlin3 in both inside-out and outside-in events independent of each other. In contrast to the study by Harburger et al. (16), Kindlin3 promotes, not inhibits, activation of β1 integrins. Interestingly, the consequences of Kindlin3 absence on integrin-mediated adhesion and spreading of microglia are similar to those of Kindlin3 mutations, which abolish its interaction with the integrin cytoplasmic domain. The overall phenotype of Kindlin3-knockin mice seems to be milder compared with Kindlin3 deficiency (22, 40), thereby indicating that Kindlin3 might have either integrin-independent functions or additional binding sites for integrin cytoplasmic domain. In microglia, however, cell adhesion and spreading on the ECM are almost completely abolished in both Kindlin3-knockin and K3KO cells, indicating that

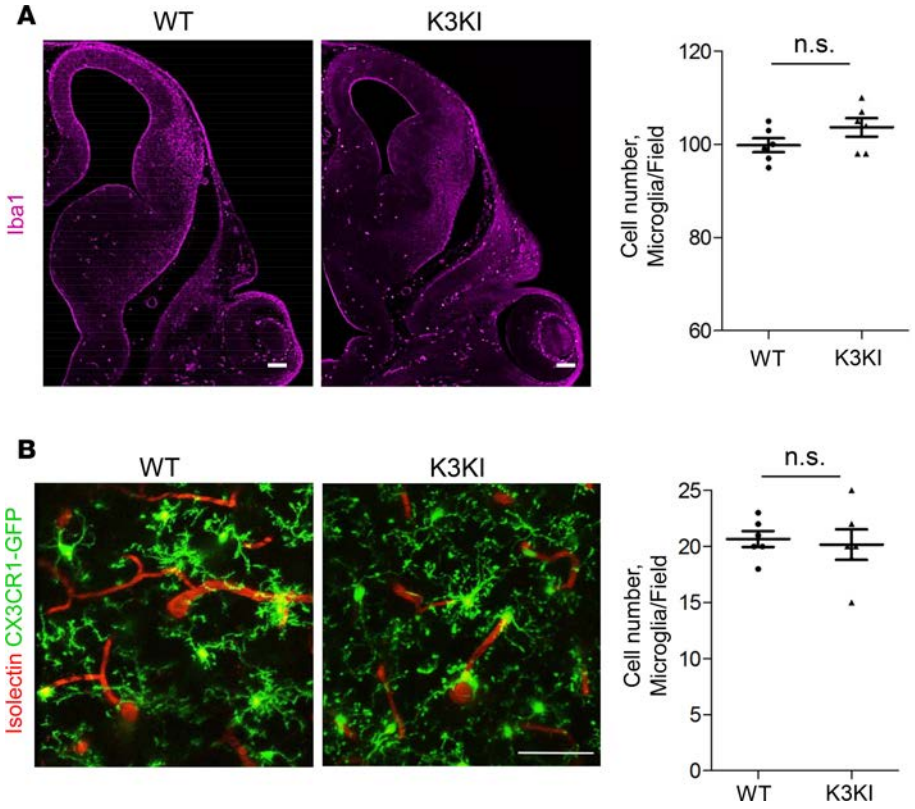

Figure 10. Kindlin3 is not required for colonization of the brain by microglial cells during development. (**A**) Cross section of day 13.5 embryos showing comparable numbers of microglia present in WT and Kindlin3 mutant knockin (K3KI) brain and eye compartments. Embryos were stained with Iba1 for microglia. Scale bar: 100 μm. The graph shows the number of microglia per field (n = 6) from 3 mice per group (mean ± SEM). (**B**) Cortical microglia in adult WT and K3KI mice expressing CX3CR1-GFP. Projection from a stack of multiphoton images, 80–100 μm below the pia, acquired through the cranial window. Blood vessels are labeled in red by fluorescently conjugated dextran. Scale bar: 50 μm. The graph shows an insignificant difference in the number of microglia (mean ± SEM, n = 6 fields from 3 mice per group). n.s. indicates no significance using 1-tailed Student's t test.

a key function of Kindlin3 in these immune cells is the regulation of integrin bidirectional signaling. The conclusion that Kindlin is a key regulator of bidirectional cell-matrix communications is in line with a recent elegant study showing severe adhesion and spreading defects of Kindlin-null embryonic fibroblast cells, where all Kindlins were genetically knocked out (17).

The severity of the defects observed in Kindlin3-knockin and -knockout microglia in vitro are very similar to those in isolated macrophages, indicating certain similarities between in vitro characteristics of these cell types. Indeed, K3KI macrophages display deficient adhesion, spreading, polarization, and migration in vitro, which are anticipated based on the known role for Kindlin3 in circulating blood cells (13, 20). For most if not all blood-derived cells, these in vitro defects are also manifested in vivo, resulting in impaired neutrophil recruitment to inflammatory sites and deficient adhesion and transmigration of monocytes and macrophage recruitment (13, 20, 41). Together, these deficiencies are responsible for known complications of Kindlin3 deficiency (or LAD-III syndrome) in humans (21, 42).

However, according to recent reports, resident brain microglia have a unique gene expression signature, which is strikingly distinct from that of any circulating immune cells, i.e., neutrophils, lymphocytes, monocytes, and tissue macrophages (from liver, kidney, lung, etc.) as well as known macrophage and microglial cell lines (23). The functional responses of microglia are also distinct from those of macrophages recruited from blood within the very same tissue (24), strongly suggesting that conclusions regarding microglia physiology cannot possibly be drawn from an analysis of monocytes/macrophages. In fact, only freshly isolated brain microglia shared some but not all markers of "real" in vivo microglia (23). Overall, these studies question the relevance of in vitro analyses of microglia functions. Indeed, we show that despite the severe defects in adhesion, cytoskeletal rearrangement and dramatically impaired migration in two different models in vitro, the lack of Kindlin3 does not affect microglial cell motility in vivo; this is in striking contrast to blood-derived macrophages. Kindlin3 appears to be absolutely dispensable for microglial relocation from the yolk sack to the CNS during embryonic development. Microglial precursors colonize the surface of the brain between E9.5 and E10.5 and later appear within the brain neuroepithelium (32). Although the precise routes and the mechanisms of developmental migration of the microglial precursors are not understood, it was proposed that microglial precursors might be mobilized to the CNS from blood, but this occurs prior to the formation of the blood-brain barrier (31). One of the suggested scenarios is that microglial precursors

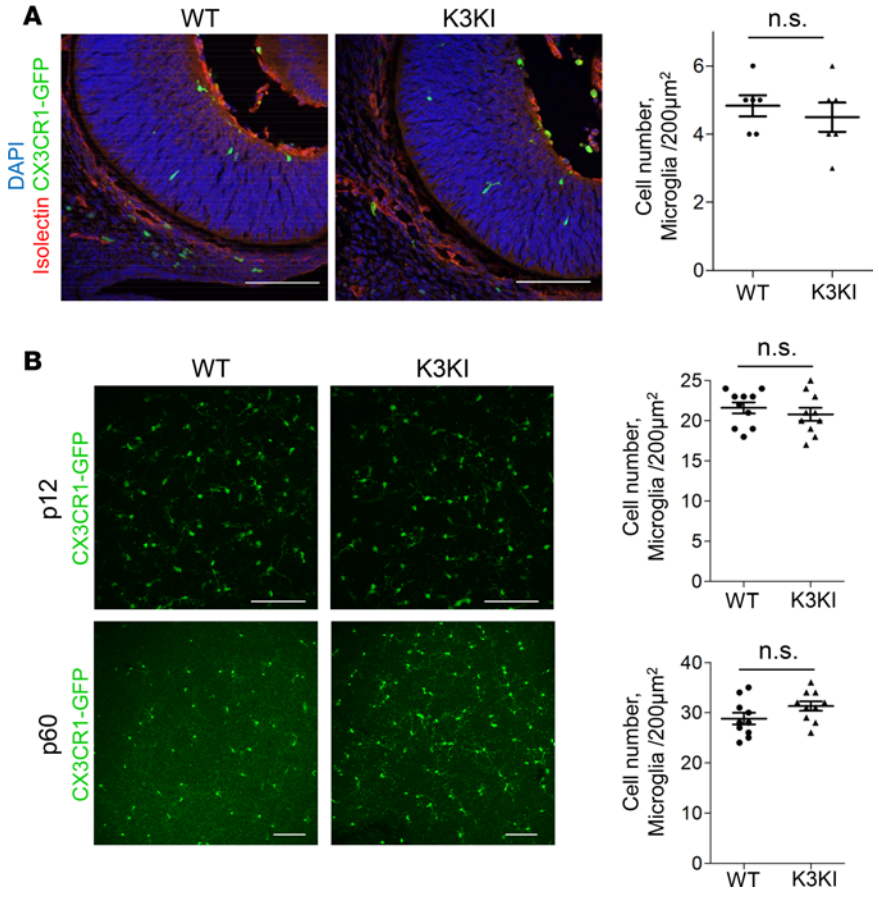

Figure 11. Kindlin3 mutant knockin microglia migrate and populate the retina, similar to WT microglia. (**A**) Cross section of E13.5 retina expressing CX3CR1-GFP stained with DAPI (blue) and isolectin (red). Scale bar: 200 μm. No significant difference was observed in microglia number, as shown by graph (mean ± SEM, *n* = 6 fields from 4 mice per group). (**B**) Confocal images of p12 and p60 whole-mount retinas from WT and K3KI mice expressing CX3CR1-GFP. Scale bar: 100 μm. The graph (right) shows an insignificant difference in number of microglia between the two groups at p12 and p60 (mean ± SEM, *n* = 10 fields from 5 mice per group). n.s. indicates no significance using 1-tailed Student's *t* test.

are still required to transmigrate through endothelium to inhabit the embryonic brain tissue, which is anticipated to be somewhat similar to macrophage recruitment (31).

The striking difference between Kindlin/integrin requirements for monocyte/macrophages migration but not for microglia seem to serve as an additional evidence of a unique physiology of resident CNS microglia. During development, microglia migrate through the brain ECM to their final destination. The mechanisms of microglial precursor motility after the entry into brain ECM are obscure. The main strategy of cell migration within the 3D matrix is believed to be dependent on cycles of integrin adhesion to ECM, MMP-dependent ECM degradation, and generation of actin-rich protrusions at the leading edge (29, 43). While MMPs were shown to be essential for migration of embryonic microglia (44), we believe this report is the first to address the role of integrin signaling. Our data show that neither distribution of CX3CR1-positive cells in brain parenchyma nor their distance from blood vessels was affected by the absence of Kindlin3-integrin function. Since Kindlin3 is an essential integrin activator in microglia, these results suggest that microglial migration within the embryonic CNS is independent of integrin signaling. An increasing number of recent studies indicate the existence of an integrin and adhesion-independent strategy of cell migration in the 3D matrix involving blebbing (45, 46). In particular, this mechanism might be applicable to certain cell types during development (47).

Thus, while recruitment of blood-derived macrophages requires Kindlin3 and integrin function, the mechanism for microglial migration during embryonic development is clearly distinct and might involve cell blebbing or any other yet unknown mechanism. Interestingly, the same is true for migration of adult microglia in chronic inflammatory disease exemplified by MS. In an MS model, microglia migrate and accumulate at the sites of demyelination. In contrast to other MS models, such as experimental autoimmune encephalomyelitis, cuprizone-induced MS involves rather limited recruitment of circulating monocytes but dramatically affects resident microglia (33). Using two different microglia markers that were shown to discriminate between microglia and infiltrated monocytes (24, 34), we demonstrate the similar degree of resident microglia redistribution and microgliosis in K3KI and WT mice, indicating that this process is also integrin independent. Thus, while there are a number of common features between resident microglia and macrophages (48), the mechanisms underlying their recruitment in pathologies are distinct. Several recent studies indicated that infiltrating monocytes but not microglia initiate a massive inflammatory response at the onset of MS (24), thereby suggesting that identification of targets and pathways that specifically affect infiltrating monocytes while preserving microglia might be used for the prevention and, possibly, treatment of MS. It appears that Kindlin3 signaling might represent such a selective target for chronic inflammatory disorders of CNS.

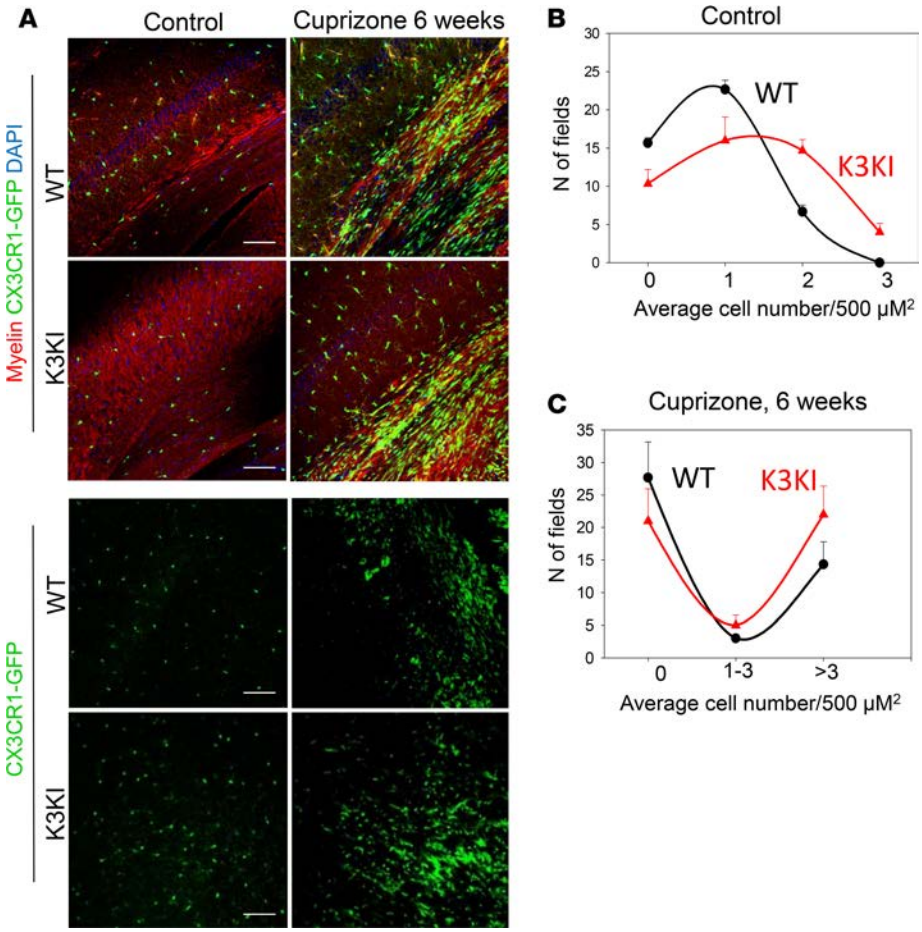

Figure 12. WT and Kindlin3 mutant knockin microglia show similar responses in a model of multiple sclerosis. (**A**) Images of brain sections stained with myelin and DAPI (top) or images of CX3CR1-GFP–expressing microglia (bottom) show the even distribution of microglia in control brains of WT/*Cx3cr1*$^{GFP/+}$ and K3KI/*Cx3cr1*$^{GFP/+}$ mice and uneven accumulation in the region of corpus callosum of brains from mice fed with cuprizone for a period of 6 weeks. Scale bar: 100 μm. (**B**) The microglia distribution pattern in healthy brains (control) of WT/*Cx3cr1*$^{GFP/+}$ and K3KI/*Cx3cr1*$^{GFP/+}$ mice is similar, with one peak with 1 cell/field within 500 μM² area. (**C**) Cuprizone induces two distinct peaks of microglia distribution representing microglia-free and microglia clusters areas.

In a model of acute injury, the lack of Kindlin3-integrin interaction delayed and impaired movement of microglial protrusions toward the site of damage, which was shown to be triggered by ATP and ADP released from damaged cells (2). ATP binding to the P2Y12 receptor is known to induce integrin activation on numerous cell types (49), a process, requiring direct Kindlin-integrin interaction. Moreover, extension of microglial processes toward the ATP source in collagen gel and in brain slices was shown to be inhibited by RGD, also indicating integrin involvement in this process (49). This study provides direct evidence that Kindlin3-mediated integrin signaling is required for timely advancement of microglial protrusions toward the site of brain damage. This process is likely to be linked to post-ligand-binding integrin signaling events, since deficient FAK phosphorylation also caused a delayed microglial response to laser-induced brain injury (50). We show that Y397 FAK phosphorylation upon integrin ligation in microglia is regulated by Kindlin3's interaction with integrins. Therefore, delayed and diminished extensions of microglial processes in Kindlin3-knockin mice are likely to be a consequence of diminished post-ligand-binding events, including Y397 FAK phosphorylation. Defects in early microglial response to injury were shown to increase lesion volume and promote its spreading into the surrounding tissues (51). In addition, microglial response to injury was shown to contribute to the timely restoration of blood-brain barrier (52).

Another important function of Kindlin3 is in the formation of microglial phagosomes during later stages of brain injury response. The presence and significance of these structures is documented in several in vivo models focused on microglia, including inflammation and neurogenesis (35, 37). Phagosome formation is known to represent a main mechanism for the engulfment of damaged neurons and the processing of cell debris (53). Therefore, the phagosomal defects caused by the lack of Kindlin3-integrin binding might delay the removal of damaged tissue, which, in turn, might later manifest in neurological complications. One should expect that microglial mobilization in acute injury is also diminished in Kindlin3-deficient human subjects. Timely isolation of injury site protects from excessive blood/plasma component leakage and microglia activation, and this timing is particularly important for Kindlin3-deficient patients charac-

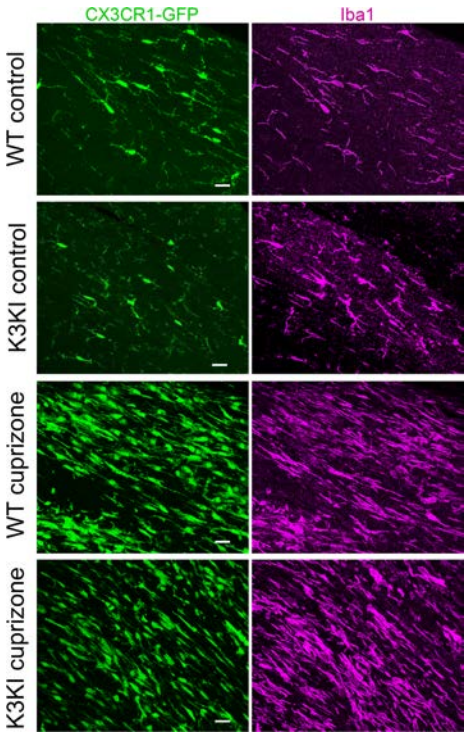

Figure 13. Normal migration and accumulation of Iba1-positive microglia of WT and K3KI mice in a multiple sclerosis model. Iba1 was immunostained on brain sections from WT/*Cx3cr1*$^{GFP/+}$ and K3KI/*Cx3cr1*$^{GFP/+}$ mice after 6 weeks of normal or cuprizone-supplemented diet. Representative confocal images of the corpus callosum area of control and cuprizone-treated brains reveal no defects in migration and accumulation of Iba1-positive cells (magenta) in K3KI/*Cx3cr1*$^{GFP/+}$ mice compared with WT/*Cx3cr1*$^{GFP/+}$ mice. Scale bar: 20 μm.

terized by impaired platelet aggregation and excessive bleeding. Therefore, our results might explain why patients with Kindlin3 deficiency displayed high incidence of brain hemorrhaging and its complications. It is important to note that Kindlin3 deficiency limited to hematopoietic cells can be successfully treated by bone marrow replacement (21). Bone marrow transplantation might promote replacement of deficient microglia with normally functioning cells of blood origin, a process rarely occurring in healthy subjects (54). Therefore, bone marrow transplantation is expected to cure not only bleeding and inflammatory defects, but also neurological complications of acute injury.

This study shows that while Kindlin3-integrin function is required for monocyte/macrophage adhesion and migration in vitro and in vivo, it is dispensable for in vivo microglial migration in development as well as in chronic inflammation of the CNS but not for the neuroprotective function of microglia during acute injury. These findings aid correct interpretation and treatment of pathological consequences of Kindlin3 deficiency in humans as well as development of new therapeutic strategies for a number of neurological diseases that require selective targeting of infiltrating monocytes/macrophages but not microglia.

Methods

Animals. K3KI mice (knockin of mutant *Kindlin3* Q597W598/AA) were described previously (40). *Cx3cr1*$^{GFP/GFP}$ mice expressing EGFP under the *Cx3cr1* promoter were obtained from the Jackson Laboratory. *Cx3cr1*$^{GFP/GFP}$ mice were crossed with WT and K3KI mice, and *Cx3cr1*$^{GFP/+}$ progeny were used for experiments. *Kindlin3*-floxed mice were custom generated by Shanghai Biomodel Organism Science and Technology Development Co LTD. Briefly, exon 2 of the *Kindlin3* gene was replaced by a fragment containing mouse WT exon 2 sequences flanked with loxP sites on both sides. A neomycin cassette was inserted into intron 2. Neo-positive ES cells were selected for generation of *Kindlin3*-floxed mouse strain. Specific integration of targeted DNA fragments was verified by Southern blot and quantitative PCR with a probe for the inserted Neo gene. The *Kindlin3*-floxed mice were crossed with *Cx3cr1*-Cre mice obtained from the Jackson Laboratory to generate K3KO mice.

Peritonitis model, macrophage isolation, and migration. Mice were injected with 0.5 ml sterile 4% thioglycollate solution into the peritoneal cavity. After 72 hours, peritoneal macrophages were collected in cold PBS containing 2 mM EDTA. Red blood cells were lysed using RBC lysis buffer (eBioscience), and macrophages were counted in hemocytometer.

For in vitro migration assay, 5×10^4 peritoneal macrophages from WT and K3KI mice were seeded per well, which was coated with 10 μg/ml fibronectin using the Oris Universal Cell Migration Assay plate (Platypus Technologies) according to the manufacturer's protocol. After 48 hours, cells were stained with calcein, and cell migration was quantified by measuring fluorescence intensity in the exclusion zone. Kindlin3-deficient peritoneal macrophages were transfected with 5 μg each of EGFP-control vector or EGFP-Kindlin3 vector as described previously (21). The images were taken 48 hours after transfection.

Cuprizone diet. Eight-week-old WT and K3KI mice were fed with 0.2% wt/wt cuprizone (Teklad) mixed with regular chow for 6 weeks. Control animals were fed regular chow. The feed of both experimental and control mice was changed every 3 days, and food intake was monitored. After 6 weeks on the diet, mice were deeply anesthetized, perfused transcardially with 4% paraformaldehyde in PBS (pH 7.4 at 4°C), and brains were isolated.

Multiphoton live imaging and laser ablation brain injury. K3KI/*Cx3cr1*$^{GFP/+}$ and WT/*Cx3cr1*$^{GFP/+}$ mice (16–20 weeks old) were imaged as previously described with minor modifications (2, 36). Briefly, mice were anesthetized and placed in the prone position in a stereotactic apparatus. A 2.0-mm diameter craniotomy over the right cortex was performed to create a "cranial window." TRITC-dextran (2.5 mg/ml, Sigma-Al-

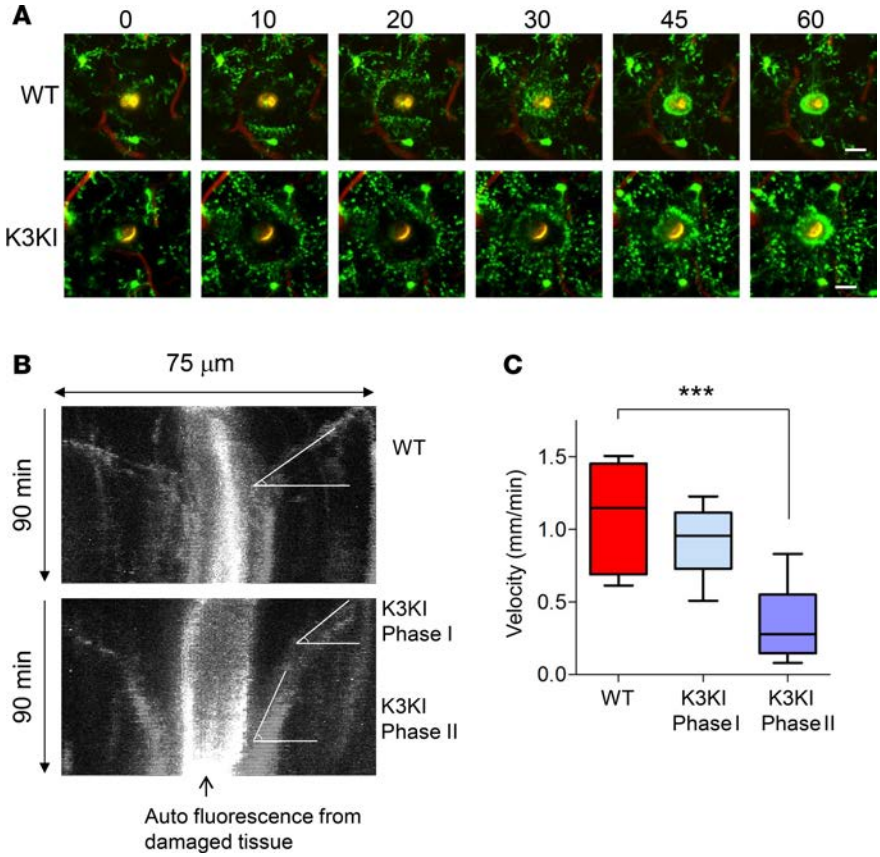

Figure 14. Kindlin3 is involved in microglial response to laser-induced brain injury. (**A**) Selected projections from a stack of multiphoton images taken 80–100 μm below the pia, acquired through the cranial window in vivo. Microglia projections labeled in green by GFP expressed under *Cx3cr1* promoter coalesce around laser injury (center). Blood vessels are labeled in red by retro-orbital injection of fluorescently conjugated dextran. Numbers above images represent time in minutes. Scale bar: 20 μm. (**B**) Representative kymographs showing dynamics of microglial processes toward the ablation site (indicated by arrow). The *x* axis represents the distance (75-μm field); the *y* axis represents the time from top to bottom (90 minutes, starting at 45 seconds after the injury). (**C**) Velocity of microglial process toward the site of injury was determined from kymographs, as described in Methods (n = 8 kymographs per group from total 6 animals). Box-and-whisker plots show median (line within box), upper and lower quartiles (bounds of box), and minimum and maximum values (bars). ***P < 0.001, 1-tailed Student's t test.

drich) was injected intravenously to outline the blood vessels. Images were acquired on a Leica TSC SP5 II confocal microscope equipped with a tunable chameleon infrared multiphoton laser (Coherent) and a ×25 water immersion objective (Leica, NA 0.95). Two hybrid-PMT (HyD) detectors (Leica) with 2 bandpass filters (525/50 nm and 585/40 nm) were used for GFP and TRITC detection, respectively. Stacks of vertical images with a step size of 2 μm at the depth of 80–100 μm below pia were collected at indicated time intervals. Microglial process movement was recorded for 10 minutes at 45-second intervals with laser at 900 nm to serve as a baseline. A laser ablation injury was then introduced with a laser powered at 720 nm for 1 second, inducing a 20 ± 0.5–μm diameter lesion. Movement of microglial processes was monitored at 900 nm for 90 minutes at 45-second intervals, followed by 4-minute intervals for the next 8 hours. Four-dimensional images (*xyzt*) were analyzed with Volocity software (BioRad). The expression of Kindlin3 in cortical microglia in adult mice was verified by immunohistochemistry.

Microglia isolation and culture. Microglial cells were isolated from brain tissue of neonatal mice and cultured as previously described (55, 56). Brain cortices of P2 mice were dissociated by resuspension in cold PBS and strained through a 70-μm net. The cells were then centrifuged and plated on a glass-bottom dish or a plastic dish and cultured for 2 to 4 weeks in DMEM/F12 with 20% FBS supplemented with nonessential amino acids. To delete the *Kindlin3* gene, microglia isolated from $K3^{lox/lox}$ mice were infected with adenovirus encoding Cre-GFP or GFP-only (University of Iowa Gene Transfer Vector Core Facility, Iowa City, Iowa, USA). Infection efficiency was confirmed by GFP expression. Cells were assayed 10 days after the infection.

Cell spreading analysis. For analysis of microglia adherent to astrocyte-deposited ECM, brain cells were seeded on glass-bottom dishes; 2 weeks later astrocytes were removed by trypsinization in the presence of 0.5 mM Ca^{2+}, as previously described (56). Microglial cells remain attached to the surface under these conditions. For Cre-mediated excision of Kindlin3 in vitro, brain cultures from *Kindlin3*-floxed transgenic mice were infected with GFP-Cre or GFP control adenoviruses 1 day after seeding. The infection efficiency was evaluated by GFP expression after 48 hours. The effectiveness of Kindlin3 deletion in microglial cells was confirmed by Kindlin3 immunostaining 10 days after the infection.

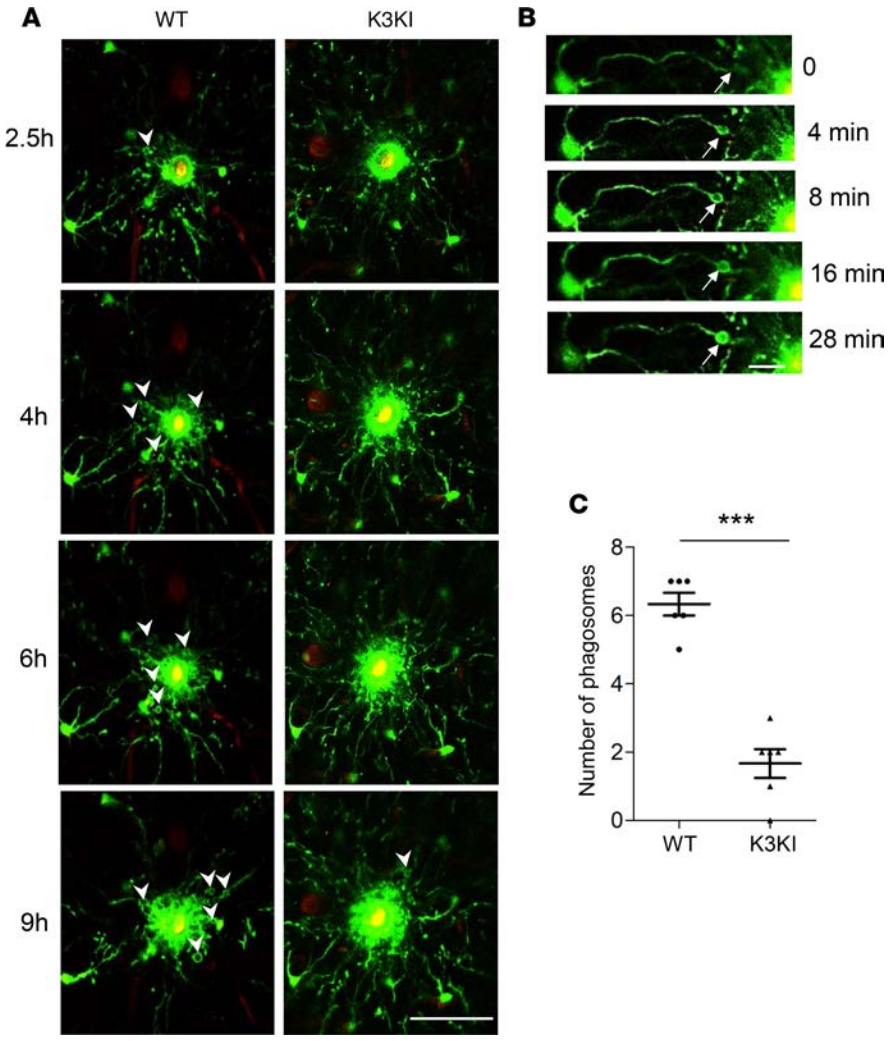

Figure 15. Kindlin3 is involved in microglial phagosome formation in proximity of injury scars. (**A**) Formation of phagosomes between 2.5 hours and 9 hours after laser-induced injury. Arrowheads indicate individual phagosomes. Scale bar: 50 μm. (**B**) Tracking of a single of phagosome (white arrows) for 30 minutes in a representative cell. Scale bar: 10 μm. (**C**) The number of phagosomes at 6 hours after injury, quantified in Z-stack image (mean ± SEM; n = 6 fields per group from total 6 animals). ***P < 0.001, 1-tailed Student's t test.

For analysis of microglial spreading on fibronectin and laminin, microglial cells were isolated from mixed glial cultures by shaking procedure as previously described (55). Microglial cells were plated in growth medium on fibronectin- (10 μg/ml) or laminin-covered (10 μg/ml) glass surfaces for the indicated time periods. For analysis of spreading in the presence of integrin stimulators, the growth medium was supplemented with C5a (10 ng/ml), fractalkine (200 ng/ml), or $MnCl_2$ (1 mM). Cell-spreading area and cell circularity were measured using ImageJ software (NIH).

Analysis of random cell migration. Mixed brain cells were cultured on glass-bottom dishes for 2 weeks. Astrocytes were then removed as described above. Microglial cells were cultured for 1 day in astrocyte-conditioned growth medium to ensure their recovery from trypsin exposure. The dishes were then placed on humidified microscopic stage with 5% CO_2 at 37°C, and differential interference contrast (DIC) microscopy time-lapse images were collected at indicated time intervals.

Analysis of chemotactic migration. Microglial cells were isolated using the shaking procedure as described above. The cells in growth medium were placed into the upper chamber of 5-μm pore Transwell inserts, precoated with fibronectin (10 μg/ml) on both sides. The medium in the bottom chamber was supplemented with C5a (10 ng/ml) or fractalkine (200 ng/ml), with or without cyclic RGD peptide (10 μM) as indicated. The cells were allowed to migrate for 5 hours and then fixed with 2% PFA. The cells on both sides of the insert were stained with DAPI reagent and Alexa-conjugated isolectin (Molecular Probes) for visualization of microglial cells. The Transwell membranes were cut out and mounted on a glass slide bottom side down. Confocal microscopy was used to take images from the upper and the lower sides of the membrane. Microglial cells were counted on each side, and the percentage of cells that migrated to the bottom surface of the membrane from the total for each field was quantified. The total number of cells for each field refers to the sum of cells on both sides of the membrane. No cells were found at the bottom of the well.

Flow cytometry. For assessment of soluble fibrinogen binding, microglial cells were isolated as described above. The cells were incubated with FITC-labeled fibrinogen and Alexa 647–conjugated anti-mouse CD11b antibody (BD Pharmingen, clone M1/70) for 30 minutes on ice in DMEM/F12 with or without $MnCl_2$ (1 mM). Microglial cells were analyzed with a 2-laser FACS Canto II flow cytometer, and data acquisition was performed with BD FACS Diva software. For assessment of integrin expression, cells were stained with Alexa 647–conjugated anti CD29/β1 integrin and FITC-conjugated anti-CD18/β1 antibodies (BD Pharmingen clones Ha2/5 and C71/16, respectively).

Immunostaining. Microglia plated on glass coverslips were fixed with 2% PFA in PBS for 20 minutes, permeabilized with 0.2 % Triton in PBS for 10 minutes, and blocked with 3% BSA and 10% goat

serum in PBS for 1 hour. The following antibodies were used for immunofluorescence: rabbit anti-Iba1 (019-19741, Wako), Alexa-conjugated rat anti-F4/80 (MCA497A488, BioRad), hamster Alexa-conjugated anti-CD29/β1 integrin (562153, BD Pharmingen, clone Ha2/5), rat Alexa-conjugated anti-CD11b/Mac1 (557960, BD Pharmingen, cloneM1/70), mouse Alexa-conjugated anti-FAK (16-233, Millipore, clone 4.47), rabbit anti-FAK pY397 (ab39967, Abcam), anti-phospho S19 Mlc2 (3671, Cell Signaling), and rat anti-GFAP (130300, Life Technologies). Rabbit polyclonal antibody to c-terminal Kindlin3 peptide ELDEDLFLQLTGGHEAF was previously described (57). Alexa-conjugated phalloidin (A12380, Molecular Probes) was used to visualize filamentous actin.

Rat monoclonal 9EG7 antibody (550531, BD Biosciences) to active ligand bound β1 integrin was used to assess β1 integrin function. For analysis of 9EG7 antibody binding, live microglial cells growing in glass-bottom dishes were incubated with 9EG7 or control rat IgG in growth medium (1.5 μg/ml) at 37°C for 5 minutes. The cells were then washed in growth medium and fixed with 2% PFA. Fluorescently conjugated goat anti-rat antibody was used as a secondary antibody.

For brain tissue staining, deeply anesthetized mice were perfused with PBS and then with 4% PFA. Brains were collected and incubated in 4% PFA overnight, followed by 48 hours of incubation in 10% sucrose solution at 4°C. The brains then were frozen with dry ice and cut into 30-μm coronal sections using cryotome (Leica CM1850 cryostat). Free-floating sections were blocked with 0.5% Triton, 10% goat serum, and 3% BSA solution in PBS overnight and stained with primary antibodies in the same solution overnight, followed by washes in PBS. The sections were then incubated with secondary Alexa-conjugated antibodies in 10% goat serum and 3% BSA solution in PBS for 1 hour at room temperature, washed, and mounted on glass slides.

For whole-mount retina staining, retinal cups were isolated and prepared as described previously (58). Enucleated eyes were fixed for 1 hour on ice in 4% PFA, rinsed with PBS, and dissected. Isolated retinal cups were fixed overnight in 4% PFA at 4°C, washed in PBS, and then blocked and permeabilized in 0.5% Triton, 10% goat serum, and 3% BSA solution in PBS for overnight. Retinas were stained with primary antibodies overnight followed by washes with PBS and then were incubated with secondary Alexa-conjugated antibodies in 10% goat serum, 3% BSA solution in PBS for 1 hour at room temperature, Alexa-conjugated isolectin was used to visualize blood vessels. After final washes in PBS, retinas were flattened and mounted on glass slides. Confocal images were obtained using a Leica SP5 confocal/multiphoton microscope.

Image analysis. Cell average fluorescent intensities were measured upon manual outlining of cells. Line average fluorescent intensity profiles were measured along the longest cell axis using ImagePro software. For measurements, cell circularity and surface areas for individual cells were analyzed with the corresponding shape descriptor functions of ImageJ software. Quantification of staining intensity was done in stacks of confocal images using Volocity software. For 3D reconstitution of confocal image stacks, Volocity software filter function was applied to reduce noise.

Migration velocity of microglia in vitro was analyzed by individual cell tracking of 12-hour time-lapse DIC image sequences in ImageJ software. Radial movement of microglial processes toward the site of laser-induced injury in vivo was analyzed by kymograph. Vertical stacks of multiphoton images were collapsed, and 90-minute time-lapse sequences of flat image projections with 45-secondsframe intervals were analyzed. A straight 75-μm line was drawn across the center of the oblation site, and kymographs were constructed with the multi-kymograph function in Fiji software. The plane of radial process movement for each experiment was analyzed from 3 different directions. Microglial process velocity was quantified from the kymograph as follows: $(x/y) \times$ pixel size (μm/px) × pixels/min.

Statistics. All histograms are expressed as mean ± SEM. One-tailed Student's *t* test was used to evaluate the statistical differences between two groups (WT vs. K3KI and WT vs. K3KO). A *P* value of less than 0.05 was considered significant.

Study approval. Experimental procedures in animals were performed in accordance with NIH guidelines on animal care, and all protocols were approved by the Animal Care Committee at Cleveland Clinic.

Author contributions

TVB and JM designed the study, analyzed the data, and wrote the manuscript. JM, ZC, TD, RMC, RM SKB, EP, SS, EFP, and BDT designed and performed the experiments. All authors discussed the results and commented on the manuscript.

Acknowledgments

This research was supported by NIH grants PO1 HL073311, and R01HL071625. We acknowledge the use of the Cleveland Clinic Imaging Core equipment and services supported by NIH Shared Instrument Grant 1S10RR026820-01. We would like to acknowledge Mira Tischenko and Huiqin Nie for their work with the animals used in this study.

Address correspondence to: Tatiana V. Byzova, Department of Molecular Cardiology, Lerner Research Institute, 9500 Euclid Avenue, Cleveland, Ohio 44195, USA. Phone: 216.445.4312; E-mail: byzovat@ccf.org.

1. Ransohoff RM, Cardona AE. The myeloid cells of the central nervous system parenchyma. *Nature*. 2010;468(7321):253–262.
2. Davalos D, et al. ATP mediates rapid microglial response to local brain injury in vivo. *Nat Neurosci*. 2005;8(6):752–758.
3. Nimmerjahn A, Kirchhoff F, Helmchen F. Resting microglial cells are highly dynamic surveillants of brain parenchyma in vivo. *Science*. 2005;308(5726):1314–1318.
4. Schafer DP, Stevens B. Microglia function in central nervous system development and plasticity. *Cold Spring Harb Perspect Biol*. 2015;7(10):a020545.
5. Li T, Zhang S. Microgliosis in the injured brain: infiltrating cells and reactive microglia both play a role. *Neuroscientist*. 2016;22(2):165–170.
6. Hanisch UK, Kettenmann H. Microglia: active sensor and versatile effector cells in the normal and pathologic brain. *Nat Neurosci*. 2007;10(11):1387–1394.
7. Milner R, Campbell IL. The extracellular matrix and cytokines regulate microglial integrin expression and activation. *J Immunol*. 2003;170(7):3850–3858.
8. Milner R, Campbell IL. The integrin family of cell adhesion molecules has multiple functions within the CNS. *J Neurosci Res*. 2002;69(3):286–291.
9. Schafer DP, et al. Microglia sculpt postnatal neural circuits in an activity and complement-dependent manner. *Neuron*. 2012;74(4):691–705.
10. Davalos D, et al. Fibrinogen-induced perivascular microglial clustering is required for the development of axonal damage in neuroinflammation. *Nat Commun*. 2012;3:1227.
11. Malinin NL, Pluskota E, Byzova TV. Integrin signaling in vascular function. *Curr Opin Hematol*. 2012;19(3):206–211.
12. Winograd-Katz SE, Fässler R, Geiger B, Legate KR. The integrin adhesome: from genes and proteins to human disease. *Nat Rev Mol Cell Biol*. 2014;15(4):273–288.
13. Malinin NL, Plow EF, Byzova TV. Kindlins in FERM adhesion. *Blood*. 2010;115(20):4011–4017.
14. Ye F, et al. Recreation of the terminal events in physiological integrin activation. *J Cell Biol*. 2010;188(1):157–173.
15. Lagarrigue F, Kim C, Ginsberg MH. The Rap1-RIAM-talin axis of integrin activation and blood cell function. *Blood*. 2016;128(4):479–487.
16. Harburger DS, Bouaouina M, Calderwood DA. Kindlin-1 and -2 directly bind the C-terminal region of beta integrin cytoplasmic tails and exert integrin-specific activation effects. *J Biol Chem*. 2009;284(17):11485–11497.
17. Theodosiou M, et al. Kindlin-2 cooperates with talin to activate integrins and induces cell spreading by directly binding paxillin. *Elife*. 2016;5:e10130.
18. Cohen SJ, et al. The integrin coactivator Kindlin-3 is not required for lymphocyte diapedesis. *Blood*. 2013;122(15):2609–2617.
19. Pluskota E, et al. Kindlin-2 regulates hemostasis by controlling endothelial cell-surface expression of ADP/AMP catabolic enzymes via a clathrin-dependent mechanism. *Blood*. 2013;122(14):2491–2499.
20. Klapproth S, et al. Minimal amounts of kindlin-3 suffice for basal platelet and leukocyte functions in mice. *Blood*. 2015;126(24):2592–2600.
21. Malinin NL, et al. A point mutation in KINDLIN3 ablates activation of three integrin subfamilies in humans. *Nat Med*. 2009;15(3):313–318.
22. Moser M, et al. Kindlin-3 is required for beta2 integrin-mediated leukocyte adhesion to endothelial cells. *Nat Med*. 2009;15(3):300–305.
23. Butovsky O, et al. Identification of a unique TGF-β-dependent molecular and functional signature in microglia. *Nat Neurosci*. 2014;17(1):131–143.
24. Yamasaki R, et al. Differential roles of microglia and monocytes in the inflamed central nervous system. *J Exp Med*. 2014;211(8):1533–1549.
25. Xu Z, Cai J, Gao J, White GC, Chen F, Ma YQ. Interaction of kindlin-3 and β2-integrins differentially regulates neutrophil recruitment and NET release in mice. *Blood*. 2015;126(3):373–377.
26. Imura T, Nakano I, Kornblum HI, Sofroniew MV. Phenotypic and functional heterogeneity of GFAP-expressing cells in vitro: differential expression of LeX/CD15 by GFAP-expressing multipotent neural stem cells and non-neurogenic astrocytes. *Glia*. 2006;53(3):277–293.
27. Swaminathan V, Waterman CM. The molecular clutch model for mechanotransduction evolves. *Nat Cell Biol*. 2016;18(5):459–461.
28. Ridley AJ, et al. Cell migration: integrating signals from front to back. *Science*. 2003;302(5651):1704–1709.
29. Vincent C, Siddiqui TA, Schlichter LC. Podosomes in migrating microglia: components and matrix degradation. *J Neuroinflammation*. 2012;9:190.
30. Sasaki Y, Ohsawa K, Kanazawa H, Kohsaka S, Imai Y. Iba1 is an actin-cross-linking protein in macrophages/microglia. *Biochem Biophys Res Commun*. 2001;286(2):292–297.
31. Ginhoux F, et al. Fate mapping analysis reveals that adult microglia derive from primitive macrophages. *Science*. 2010;330(6005):841–845.

32. Arnold T, Betsholtz C. The importance of microglia in the development of the vasculature in the central nervous system. *Vasc Cell*. 2013;5(1):4.
33. Goldberg J, Clarner T, Beyer C, Kipp M. Anatomical distribution of cuprizone-induced lesions in C57BL6 mice. *J Mol Neurosci*. 2015;57(2):166–175.
34. Lampron A, et al. Inefficient clearance of myelin debris by microglia impairs remyelinating processes. *J Exp Med*. 2015;212(4):481–495.
35. Mazaheri F, et al. Distinct roles for BAI1 and TIM-4 in the engulfment of dying neurons by microglia. *Nat Commun*. 2014;5:4046.
36. Kondo S, Okabe S. In vivo two-photon microscopy of microglia. *Methods Mol Biol*. 2013;1041:319–335.
37. Sierra A, et al. Microglia shape adult hippocampal neurogenesis through apoptosis-coupled phagocytosis. *Cell Stem Cell*. 2010;7(4):483–495.
38. Moser M, Nieswandt B, Ussar S, Pozgajova M, Fässler R. Kindlin-3 is essential for integrin activation and platelet aggregation. *Nat Med*. 2008;14(3):325–330.
39. Ye F, et al. The mechanism of kindlin-mediated activation of integrin αIIbβ3. *Curr Biol*. 2013;23(22):2288–2295.
40. Xu Z, et al. Direct interaction of kindlin-3 with integrin αIIbβ3 in platelets is required for supporting arterial thrombosis in mice. *Arterioscler Thromb Vasc Biol*. 2014;34(9):1961–1967.
41. Lefort CT, et al. Distinct roles for talin-1 and kindlin-3 in LFA-1 extension and affinity regulation. *Blood*. 2012;119(18):4275–4282.
42. Svensson L, et al. Leukocyte adhesion deficiency-III is caused by mutations in KINDLIN3 affecting integrin activation. *Nat Med*. 2009;15(3):306–312.
43. Schmidt S, Friedl P. Interstitial cell migration: integrin-dependent and alternative adhesion mechanisms. *Cell Tissue Res*. 2010;339(1):83–92.
44. Kierdorf K, et al. Microglia emerge from erythromyeloid precursors via Pu.1- and Irf8-dependent pathways. *Nat Neurosci*. 2013;16(3):273–280.
45. Tozluoglu M, Mao Y, Bates PA, Sahai E. Cost-benefit analysis of the mechanisms that enable migrating cells to sustain motility upon changes in matrix environments. *J R Soc Interface*. 2015;12(106):20141355.
46. Paluch EK, Raz E. The role and regulation of blebs in cell migration. *Curr Opin Cell Biol*. 2013;25(5):582–590.
47. de Lucas B, Bernal A, Pérez LM, San Martín N, Gálvez BG. Membrane blebbing is required for mesenchymal precursor migration. *PLoS One*. 2016;11(3):e0150004.
48. Gautier EL, et al. Gene-expression profiles and transcriptional regulatory pathways that underlie the identity and diversity of mouse tissue macrophages. *Nat Immunol*. 2012;13(11):1118–1128.
49. Ohsawa K, et al. P2Y12 receptor-mediated integrin-beta1 activation regulates microglial process extension induced by ATP. *Glia*. 2010;58(7):790–801.
50. Choi I, et al. LRRK2 G2019S mutation attenuates microglial motility by inhibiting focal adhesion kinase. *Nat Commun*. 2015;6:8255.
51. Hines DJ, Hines RM, Mulligan SJ, Macvicar BA. Microglia processes block the spread of damage in the brain and require functional chloride channels. *Glia*. 2009;57(15):1610–1618.
52. Lou N, Takano T, Pei Y, Xavier AL, Goldman SA, Nedergaard M. Purinergic receptor P2RY12-dependent microglial closure of the injured blood-brain barrier. *Proc Natl Acad Sci U S A*. 2016;113(4):1074–1079.
53. Jin X, Yamashita T. Microglia in central nervous system repair after injury. *J Biochem*. 2016;159(5):491–496.
54. Okonogi N, et al. Cranial irradiation induces bone marrow-derived microglia in adult mouse brain tissue. *J Radiat Res*. 2014;55(4):713–719.
55. Giulian D, Baker TJ. Characterization of ameboid microglia isolated from developing mammalian brain. *J Neurosci*. 1986;6(8):2163–2178.
56. Saura J, Tusell JM, Serratosa J. High-yield isolation of murine microglia by mild trypsinization. *Glia*. 2003;44(3):183–189.
57. Meller J, et al. Novel aspects of Kindlin-3 function in humans based on a new case of leukocyte adhesion deficiency III. *J Thromb Haemost*. 2012;10(7):1397–1408.
58. Pitulescu ME, Schmidt I, Benedito R, Adams RH. Inducible gene targeting in the neonatal vasculature and analysis of retinal angiogenesis in mice. *Nat Protoc*. 2010;5(9):1518–1534.